Distribution Agreement

In presenting this thesis as a partial fulfillment of the requirements for a degree from Emory University, I hereby grant to Emory University and its agents the non-exclusive license to archive, make accessible, and display my thesis in whole or in part in all forms of media, now or hereafter now, including display on the World Wide Web. I understand that I may select some access restrictions as part of the online submission of this thesis. I retain all ownership rights to the copyright of the thesis. I also retain the right to use in future works (such as articles or books) all or part of this thesis.

Michelle Garrison April 12, 2022

Synthesis and Biological Investigation of Natural Product-Inspired Antimicrobial Compounds

by

Michelle Garrison

William Wuest, Ph.D.
Advisor

Department of Chemistry

William Wuest, Ph.D.

Advisor

Frank McDonald, Ph.D.

Committee Member

John Lysaker, Ph.D.

Committee Member

2022

Synthesis and Biological Investigation of Natural Product-Inspired Antimicrobial Compounds

By

Michelle Garrison

Dr. William Wuest

Advisor

An abstract of
a thesis submitted to the Faculty of Emory College of Arts and Sciences
of Emory University in partial fulfillment
of the requirements of the degree of
Bachelor of Science with Honors

Department of Chemistry

2022

Abstract

Synthesis and Biological Investigation of Natural Product-Inspired Antimicrobial Compounds
By Michelle Garrison

Antibiotic resistance poses an alarming threat to public health. Over time, bacteria continually evolve and develop drug resistance, evading commonly used antibiotics. It is therefore necessary to synthesize novel antimicrobials with unique mechanisms of actions to overcome this problem. Compounds isolated from nature often show unique abilities to this end, and can be synthesized and modified to create new therapeutic agents.

Quaternary ammonium compounds (QACs) comprise an important class of molecules due to their widespread use as antiseptic agents both commercially and in the household. Tricepyridinium bromide, a QAC natural product with a unique structure, showed promising inhibitory activity against *S. aureus* upon its initial isolation, prompting our investigation into its biological activity and mechanism of action. An efficient and reproducible synthetic route was devised to access tricepyridinium bromide as well as four different analogues. The resulting products then underwent biological analysis, and their inhibitory activity was compared to that of two commercially available QACs: cetylpyridinium chloride (CPC) and benzalkonium chloride (BAC). It was found that tricepyridinium and select analogues showed selectivity towards gram-positive bacteria while also maintaining little to no hemolytic activity. In addition, the relationship between tricepyridinium and the QacR transcription factor responsible for regulating a QAC resistance pathway was investigated using molecular modeling. Our studies showed that tricepyridinium and shorter-chain N-alkyl analogs may preferentially bind to this transcription factor, thereby conferring QAC resistance.

We also sought to better understand the potential bioactivity of several newly isolated lumazine peptides, one of which possessed isonitrile functionality. Isonitriles are unique in their ability to chelate metal, which we hypothesized could work as a way to attenuate bacterial virulence. Our current work focuses on synthesizing several isonitrile-functionalized lumazine peptides with the intention of studying the effects of this functional group on the bioactivity of these molecules.

Synthesis and Biological Investigation of Natural Product-Inspired Antimicrobial Compounds

By

Michelle Garrison

Dr. William Wuest

Advisor

A thesis submitted to the Faculty of Emory College of Arts and Sciences
of Emory University in partial fulfillment
of the requirements of the degree of
Bachelor of Science with Honors

Department of Chemistry

2022

Acknowledgements

I would like to extend my sincere gratitude and appreciation to the members of my committee, Dr. William Wuest, Dr. Frank McDonald, and Dr. John Lysaker who took the time out of their busy schedules to support my work.

To Dr. Wuest: I want to thank you for your support of my research and education throughout my time at Emory. Your commitment to helping me grow as a student has allowed me to develop as a scientist and person, and has been instrumental in helping me to achieve my academic and professional goals.

To Dr. McDonald: Your dedication and passion for teaching has had a pivotal influence on my educational career at Emory. Being in your organic chemistry class during my first year at Emory helped to cultivate my love for the subject and helped me point me to my current area of research, and for that I am incredibly grateful.

To Dr. Lysaker: Being your student was truly a privilege, and your class proved to be one of the most impactful courses I have ever been a part of. Thank you for your helping me to grow as a student and helping me to deepen my appreciation for the discipline of philosophy.

Finally, I would also like to thank my graduate student mentor, Andrew Mahoney. Your endless guidance, advice, and encouragement allowed me to grow in confidence as throughout my time at Emory, and your bright spirit taught me to approach my work with optimism and enthusiasm each day.

Table of Contents

Figures, Schemes, and Tables

1. Antibiotics: The Story So Far

1.1 Bacteria and Antibiotics in Everyday Life

Humans coexist with countless microbes, with trillions of bacteria populating the human gut, skin, and oral cavities. Most of the time, these bacteria pose no threat or are even beneficial to human health. For example, approximately 100 trillion bacteria comprise what is known as the microbiome in the human gastrointestinal tract.[1] This microbe ecosystem in the digestive tract provides essential nutrients, aids in the synthesis of vitamin K, allows for cellulose digestion, and promotes angiogenesis and enteric nerve function.[2] Bacteria can also protect mucosal tissues by preventing harmful antigens from entering the body. However, bacteria can also be pathogenic, causing diseases including meningitis, pneumonia, and tuberculosis. In these cases, antibiotic medication is necessary in order to clear the infection and prevent further disease progression. The development of penicillin in 1928 represented a major turning point in our ability to treat illnesses caused by bacteria, ushering in a new era dominated by the use of antibiotics.[3] Besides their utility as oral and intravenous medications for bodily infection, antibiotic compounds are also present in surface disinfectants, killing harmful bacteria both in hospitals and everyday households.

1.2 The Antibiotic and Bacterial "Arms Race"

Antibiotics have historically been used a means to kill pathogenic bacteria in patients before progressing to become a more serious infection. However, as the use of antibiotics became more common, this introduced the issue of bacterial resistance. While a particular strain of bacteria may start out as sensitive to an antibiotic, many bacteria possess variations in their genetic code that render them resistant to an administered antibiotic. Since many of the

antibiotics used today are either natural products or derived from natural products, variations in the genetic code of bacteria may be the result of natural defense mechanisms against these molecules. Resistant bacteria that are unaffected by a particular antibiotic then survive, multiply, and transfer genetic information to new bacteria, thus leading to a population of bacteria that is unresponsive to the originally administered treatment.[4] Some common mechanisms by which bacteria are able to develop resistance to antibiotics are through efflux pumps that push small molecules out of the cell, modification of the drug binding site, and degradation of the antibiotic.[5] When antibiotics are prescribed unnecessarily or a course of antibiotics is left unfinished by the patient, this accelerates the cycle of the evolution of bacteria, leading to the evolution of hyper-resistant bacteria known as "superbugs." Further, the prescription of broad spectrum antibiotics also threatens the beneficial bacteria that inhabit the human body, thereby upsetting the natural microbiome of beneficial microorganisms.

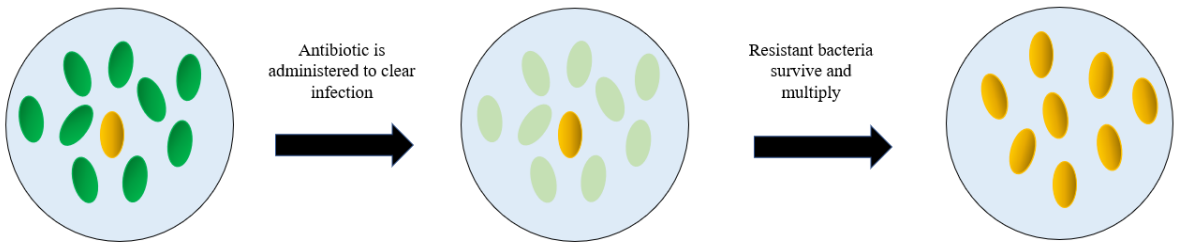

Figure 1.2.1. Evolution of antibiotic-resistant bacteria

The emergence of methicillin-resistant *Staphylococcus aureus* (MRSA) serves as an example of the harms caused by continuous bacterial evolution. *Staphylococcus aureus* is a species of bacteria that most commonly causes skin infections, but in some cases, can cause

pneumonia and sepsis. MRSA is especially prevalent in healthcare settings. Notably, the CDC states that approximately 5% of patients in U.S. hospitals carry this bacteria somewhere on their nose or skin.[6] Since the use of methicillin in 1960, *S. aureus* has developed resistance to multiple antibiotics, which has led the CDC to list MRSA as a "serious threat" to public health.[7] Resistance to antibiotics is not limited to oral and intravenous medication, and is also an issue that is exacerbated by widespread use of antibacterial surface disinfectants. The onset of the COVID-19 pandemic also brought the usage of surface antiseptics to the public eye. One key ingredient in the common disinfectant, Lysol, is benzylalkonium chloride, which is a quaternary ammonium compound (QAC) designed to kill bacterial through membrane permeabilization. Widespread use of these surface disinfectants places selective pressure places selective pressure on bacteria to evolve resistance mechanisms to these antimicrobials, further exacerbating the problem of antibiotic resistance.[8]

The prevalence of antibiotic resistance is now a pressing crisis that must be addressed. According to the CDC, over 2.8 million antibiotic-resistant infections occur annually in the United States alone. Worldwide, approximately 4.95 million deaths were attributed to drug-resistant infections in 2019.[9] Further, the World Health Organization reported that antimicrobial resistance is one of the top 10 global health threats facing the world. This urgent need to treat antibiotic-resistant infections has resulted in an "arms race" to develop novel drug therapies that keep pace with the rapid evolution of bacteria. Despite this threat, the pace of development of novel antibiotics lags behind the rapid evolution of bacteria. In 2019, the WHO identified just 32 new antibiotics in clinical development. These numbers illustrate the ongoing need for research

and development of novel antibiotics that are equipped to keep pace with rapid bacterial evolution.

1.3. Fighting Superbugs

The Wuest lab aims to develop novel antimicrobials by employing methods in synthetic organic chemistry and microbiology. The prevalence of antibiotic resistance highlights the urgent need for new antibiotics with unique structures and mechanisms of action. By synthesizing and studying the activity of novel compounds with the ability to serve as antibiotics, this research can serve not only to produce new antimicrobials, but also better understand the ways in which bacteria are able to evade traditional antibiotics. Compounds isolated from nature often show unique abilities to serve as antimicrobials with diverse mechanisms of actions. Several major classes of commonly-used antibiotics are derived from natural sources. For example, pencillins, derived from the mold *Pencillum notatum* inhibit cell wall biosynthesis, tetracyclines, derived from the bacterium *Micromonospora purpurea* inhibit ribosomal synthesis through protein binding, and rifamycins, derived from the bacterium *Amycolatopsis rifmycinia* bind to prokaryotic RNA polymerase to prevent synthesis. In the effort to produce new antibiotics that operate with novel mechanisms of action, we can look to nature for inspiration. In the laboratory, unique chemical structures inspired by nature can be replicated and modified to create analogues of the natural products in the laboratory using synthetic organic chemistry. These newly developed compounds can then be evaluated for biological activity against a number of clinically-relevant strains of bacteria.

2. Tricepyridinium Bromide Inspired QACs

2.1 Novel QAC Discovery

Quaternary ammonium compounds (QACs) are a nitrogen-containing class of molecules characterized by a permanent positive charge, as well as a hydrophobic alkyl portion. QACs are widely used as surface disinfectants, both in household and clinical settings.[10] The amphipathic nature of these molecules allows for the disruption of bacterial cell membranes, thus leading to cell lysis and death.[11] The frequent use of antimicrobial cleaners poses the issue of bacterial resistance, creating the need for novel agents capable of killing bacteria while maintaining low eukaryotic toxicity. One such compound, tricepyridinium bromide, showed promise to this end. Tricepyridinium bromide was first isolated from the *E. coli* cultures marine sponge, *Discodermia calyx* in 2017.[12] In its original isolation study, tricepyridinium bromide showed biological activity against *S. aureus* and the fungus *Candida albicans*, which prompted our investigation into this natural product as well as several analogues.

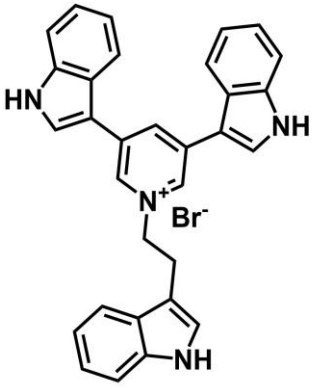

Microorganism	MIC (μg/mL)
Bacillus cereus	0.78
Staphylococcus aureus	1.56
Candida albicans	12.5
Escherichia coli	>100

Figure 2.1.1. Structure of tricepyridinium bromide and reported biological activity by Okada et al.

2.2 Proposed Mechanism of Action and Analogue Design

One common feature of QACs is their ability to perturb cell membranes, which can be attributed to the amphipathic nature of these compounds. This feature typically results in strong activity against gram-positive bacteria, but typically renders them ineffective against gram-negative bacteria due to their additional outer membrane. The structure of tricepyridinium bromide is unique in that there is no strongly nonpolar region of the molecule, which informed our hypothesis regarding its potential mechanism of action. We proposed that tricepyridinium bromide could function in a similar manner to a known QAC and cell perturbing agent, cetylpyridinium chloride (CPC) through membrane permeabilization. The planar nature of tricepyridinium bromide and its structural similarity to ethidium bromide also led us to propose a competing hypothesis - that tricepyridinium bromide may function as a DNA intercalator, thereby disrupting the bacterial cell's transcription process as well as DNA replication during cell division, ultimately leading to cell death.

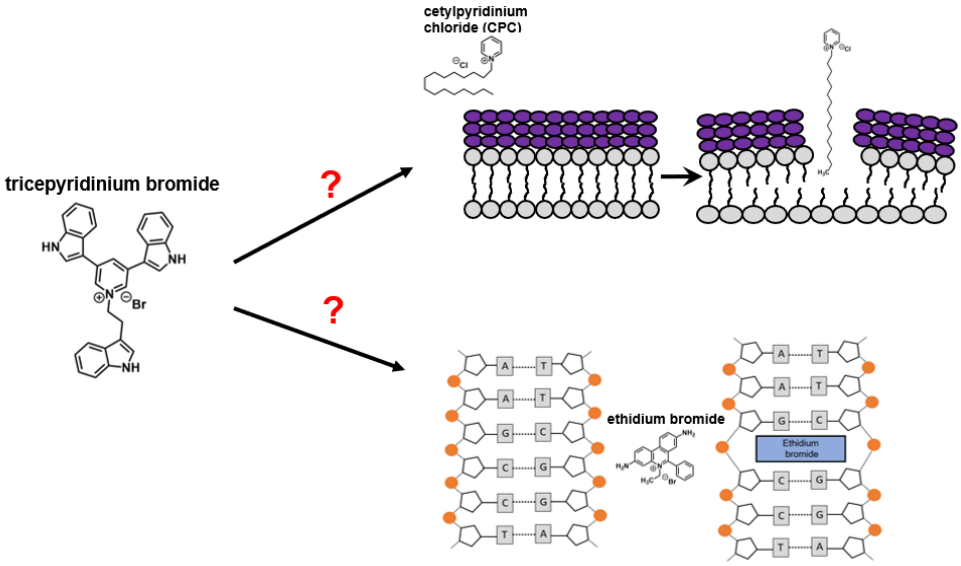

Figure 2.2.1. Proposed mechanisms of action for tricepyrindium bromide.

The design for the analogue library was fueled both by our hypothesized mechanism of action as well as previous studies of the activity of tricepyridinium bromide. Analogues synthesized by Okada et al. showed that removal of one or both of the indole moieties resulted in a significant decrease in biological activity against *Bacillus cereus* and *Staphylococcus aureus*. Strong biological activity, with minimum inhibitory concentrations (MICs) of 1.56 uL/mL for both *B. cereus* and *S. aureus* were found with the addition of an ethyl alkyl chain at the quaternary center. As a result of the findings, the goals for our analogue library focused on modification at the quaternary nitrogen.

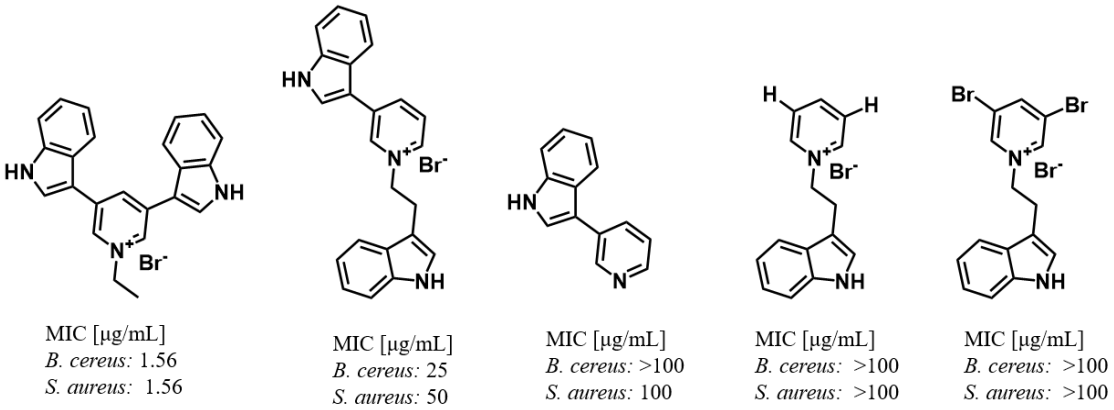

Figure 2.2.2. Previously synthesized tricepyrdinium bromide analogues and reported MICs against *B. cereus* and *S. aureus*.

Previous work on QACs from members of the Wuest lab indicated that alkyl chain lengths of 10-14 carbons are optimal for cell membrane perturbation.[13] Thus, to test our hypothesis that these compounds function through disruption of the membrane, we aimed to produce analogues with alkyl chain lengths of 10, 12, and 14 carbons, in addition to the previously synthesized ethyl analogue and natural product.

2.3 Synthesis

Our effort to synthesize tricepyridinium bromide and our desired analogues began by utilizing a previously reported route toward the natural product from Okada et al. However, due to low levels of reproducibility, we devised a new synthetic route. We sought to synthesize our analogues through a key coupling reaction of indole and pyridine. A Suzuki coupling was chosen for its versatility and broad applicability. While the pyridine precursor, 3,5-dibromopyridine, is commercially available, the indole precursor, indole-3-boronic acid pinacol ester, had to be

synthesized. The synthesis of this compound began with a base-catalyzed one-pot iodination/Boc protection of indole. We originally tried to begin this synthesis with a Boc protection of indole followed by a bromination. However, when we reached the borylation step, we found that the borylation of the Boc protected bromoindole did not achieve the desired product. Because iodine is a better leaving group than bromine, we expected that borylation could be achieved more easily using an iodinated indole. We found that the one-pot iodination/Boc protection of indole gave a better yield and allowed us to combine the first two steps of the synthesis with only one purification. Borylation of the 3-iodoindole was achieved by reacting the material with n-butyllithium and 2-isopropoxy-4,4,5,5-tetramethyl-1,3,2-dioxaborolane. This material was then used for a double Suzuki coupling using cesium carbonate, palladium-tetrakis(triphenylphosphine), and 3,5-dibromopyridine. To deprotect the nitrogen indoles on this compound, the product of the di-Suzuki coupling was then reacted with excess trifluoroacetic acid. We also tested the deprotection reaction using excess hydrogen chloride, but this reaction proceeded with a poor yield compared to the trifluoroacetic acid. The pyridine nitrogen was then quaternized with various alkyl bromides in an S_N2 reaction. Tricepyridinium bromide as well as four analogues were synthesized in six steps with an overall yield of 26-33% (Scheme 1).[14]

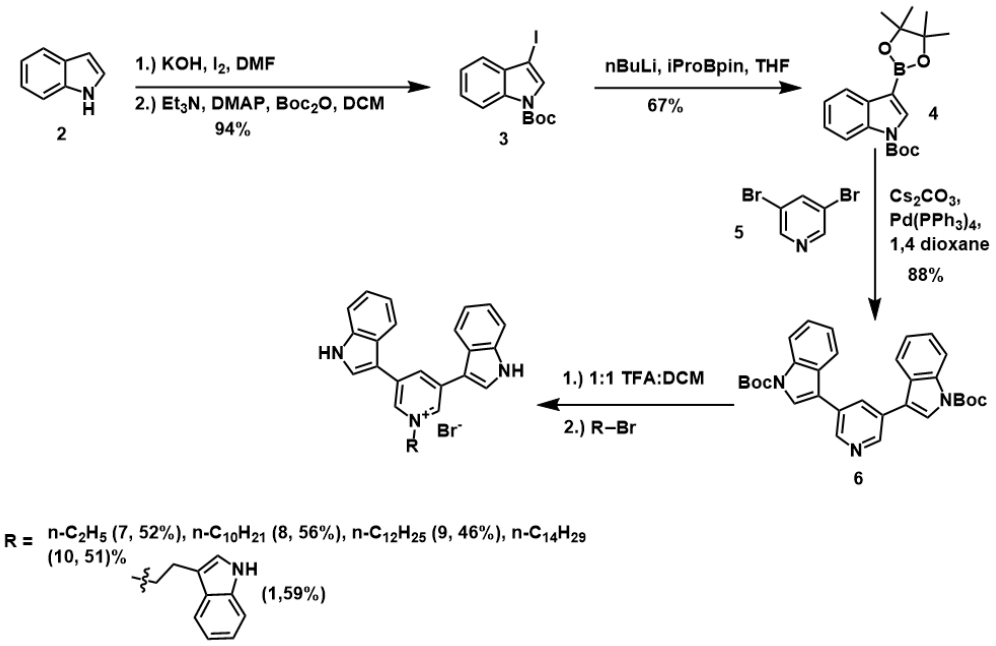

Scheme 2.3.1. Methods towards the synthesis of tricepyridinum bromide and analogues.

2.4. Biological Evaluation

After the synthesis of tricepyrindium bromide and its analogues, we then investigated the biological activity of these compunds. First, a hemolysis assay was performed in order to study toxicity of our newly-synthesized with regards to ovine erythrocytes.[15] Compounds were serially-diluted, incubated in sheep's blood for one hour, then centrifuged. To determine the concentration of lysed cells, the supernatant was removed and subjected to optical density measurements. The tested compounds exhibited low levels of eukaryotic toxicity, particularly in comparison to CPC (Table 1). This low level of in hemolytic toxicity compared to CPC suggests that tricepyridinium bromide may not function strictly via cell membrane pertubation, as membrane pertubers tend to show higher levels of hemolysis.

Table 1. Hemolytic activity of cetylpyridinium chloride (CPC) and N-alkyltricepyridinium compounds.

Compound	CPC	1	7	8	9	10
LC20 [μM]	16	125	250	125	125	125

Table 2.4.1. Hemolytic activity of CPC and N-alkyltricepyridinium compouds.

Tricepyrdinium bromide and its analogues were then tested against a panel of bacteria that included *Streptococcus mutans* (UA159), *Pseudomonas aeruginosa* (PAO1) and three strains of *Staphylococcus aureus* (the methicillin-susceptible strain SH1000, a strain with community-acquired methicillin resistance USA300, and a strain with hospital-acquired methicillin resistance ATCC33591 which harbors QAC-resistance genes). *S. mutans* is an oral pathogen and target of CPC, and *P. aeruginosa* and *E. coli* are gram-negative bacteria. These particular strains of bacteria were selected because we wanted to test if our compounds were selective for gram-positive bactera (which would provide evidence for a membrane-perturbation mechanism of action.)

Table 2. Minimum inhibitory concentration data (μM) for all N-alkylpyridinium compounds, cetylpyridinium chloride (CPC), and benzalkonium chloride (BAC). All numbers shown are the average of three replicates.

Compound	*S. mutans* UA159	S. aureus SH1000	*S. aureus* USA300	*S. aureus* ATCC33591	*P. aeruginosa* PAO1	*E. coli* MC4100
CPC	1	0.5	1	1	250	32
BAC	1	2	4	4	125	64
1	4	2	4	16	>250	>250
7	125	32	64	250	>250	>250
8	2	16	16	16	>250	>250
9	8	32	32	32	>250	>250
10	32	64	64	64	>250	>250

Table 2.4.2. MICs for N-alkylpyridinium compounds, CPC, and BAC.

The results of this biological testing showed that tricepyridinium bromide had a comparable ability with CPC and BAC to inhibit the growth of *S. mutans* and *S. aureus*, while compound 8 was the most potent synthetic analgoue. With analogues 9 and 10, a decrease in the activity of the compounds against these *S. mutans* and *S. aureus* was observed with increased alkyl chain length. All tested compounds showed selective biological activity towards gram-positive bacteria, which typically suggests that the molecule functions through membrane permeabilization. However, it was notable that compound 8 showed a greater level of selectivity towards the inhibition of *S. mutans* whereas CPC showed no such difference. These observations therefore leave the mechanism of action of the molecule unclear. On the one hand, tricepyridinium bromide and analogue 8 may function via membrane perturbation given its activity towards gram-postive bacteria. However, membrane-active compounds typically lead to cell lysis, which was not the case with our compounds as evidenced by our hemolysis studies.

Further, tricepyridinium bromide does not have a strongely non-polar region, and increasing the length of the alkyl chain on our analogues decreases biological activity. These findings leave open the possibility for another mechanism of action besides membrane perturbation, such as disruption of transcription and DNA replication via DNA intercalation.

In compounds 1 and 7, we observed a signficantly higher MIC in the methicillin-resistant *S. aureus* strain (ATCC3359) compared methicillin-susceptible strain of *S. aureus* (SH1000), whereas our long-chain analogues showed no difference significant difference in activity against these strains. This observations suggested that the methicillin-resistant *S. aureus* strain ATCC3359 had some resistance to compounds 1 and 7 in particular. In order to better understand these findings, additional molecular modeling studies performed by Andrew Mahoney, a graduate student in the Wuest lab, elucidated the relationship between compounds 1 and 7 and the QAC-efflux pump, QacC. Bacterial strain ATCC33591 (MRSA) is known to circumvent QACs through the efflux pump, QacC. This gene is regulated by the transcription factor, QacR. When a QAC binds to this transcription factor, the complex dissociates from the DNA and allows for the transcription of QacC, and thus promotes efflux of the QAC from the bacterial cell. Computional modeling showed that compounds 1 and 7 had the strongest predicted binding affinities to QacR. Thus, this increased binding affinity could account for the decrease in inhibitory activity against MRSA due to its ability to promote the transcription of genes that efflux QACs from the cell.

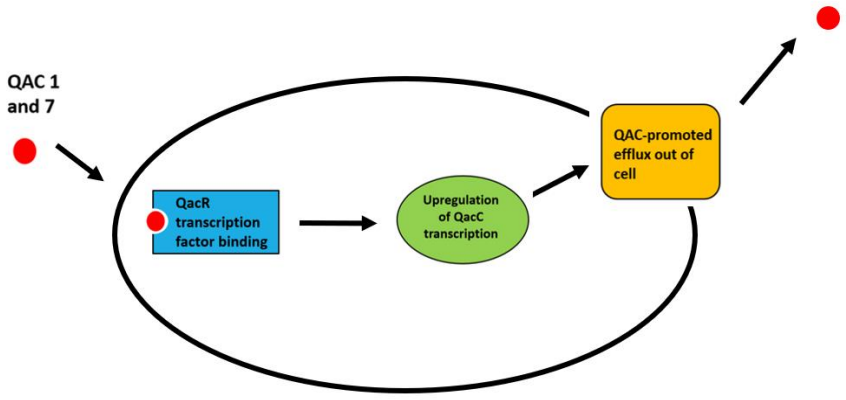

Figure 2.4.3. Proposed QAC efflux mechanism based on molecular modeling studies.

2.5. Outcomes

In summary, we were successful in devising a more easily reproducible route towards the synthesis of tricepyridinium and N-alkyl analogues. Further, we demonstrated that the natural product and compound 8 showed comparable inhibitory activity to known antibiotics, and was particularly effective against *S. mutans*. In addition, these compounds showed minimal hemolytic actiity. Finally, we were able to provide further insight into the mechanisms of QAC-efflux pump mediated QAC resistance through molecular modeling studies.

3. Lumazine Peptides

3.1. Discovery and Biological Significance

In the continued search for novel antimicrobial agents, one class of molecules called lumazine peptides showed potential as an area of research. In an isolation study published in June 2020 from the Cao Lab at the University of Hawaii, 5 new lumazine peptides were isolated from the Hawaiian fungus, *Aspergillus flavipes*.[16]

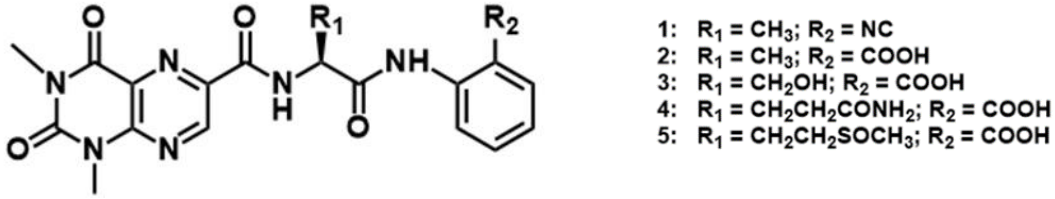

Figure 3.1.1. Lumazine peptides 1-5, isolated from *Aspergillus flavipes.*

Lumazines closely resemble the structure of pterins, which are known to have several biologically important functions, including antiviral, anticancer, and antimicrobial activity.[17]

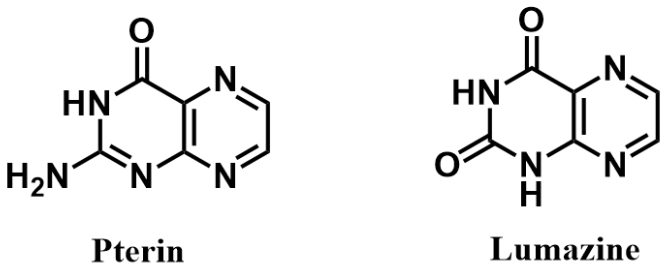

Figure 3.1.2. General structure of pterins and lumazines.

Currently, knowledge about the potential bioactivity of lumazines and lumazine peptides remains largely unexplored. Colistin and polymyxin B are two examples of peptides that function as antibiotics. These compounds exist as cationic, cyclic polypeptide antibiotics and are particularly active against gram-negative bacteria via permeabilization of the outer bacterial membrane.[18]

One particularly notable feature of the isolated natural products was the presence of a naturally occurring isonitrile functionality in compound 1. Isonitriles differ from nitriles in that they are connected to the carbon skeleton by the nitrogen rather than the carbon.[19] They exist in two different resonance structures: one with a double bond between the nitrogen and carbon and another with a triple bond. Previous research studying isonitrile-functionalized molecules has shown that this functional group has the ability to bind transition metals, particularly copper.[20] Copper is a key element for bacterial life, and is used as a cofactor or catalyst in many biological processes in methanobacteria.[21] More recent work has also shown that copper is important in enzymatic function in the more clinically relevant bacterial species, *Streptomyces*. Further, the diisonitrile compound, SF2768 was found to function as a chalkophore, meaning that this small molecule was able to bind and mediate the bacterial acquisition of copper.

Isonitrile-functionalized antibiotics also have important known clinical applications. The first discovered naturally occurring isonitrile was xanthocillin, which was isolated in 1950. Xanthocillin is effective as a broad spectrum antibiotic against gram-positive and gram-negative bacteria, although its mechanism of action is not well understood. The biological activity of xanthocillin is particularly notable because of its bioactivity against gram-negative bacteria, which have a higher barrier to permeability due to their double membrane. Recent work from

Huber et al. studying the mechanism of action of xanthocillin attributed its biological activity to its ability to bind regulatory heme, which disrupts its binding to important hemoproteins and thus impairs heme biosynthesis.[22] As a result, heme biosynthesis becomes unregulated and increases in the bacterial cell, which then leads to disruptions of the electron transport chain and an increase in reactive oxygen species. Given the precedent for peptides to serve as antibiotics, unique biological activity of isonitriles, and the limited number of naturally occurring isonitriles, we sought to explore the potential bioactivity of isonitrile-functionalized lumazine peptides.

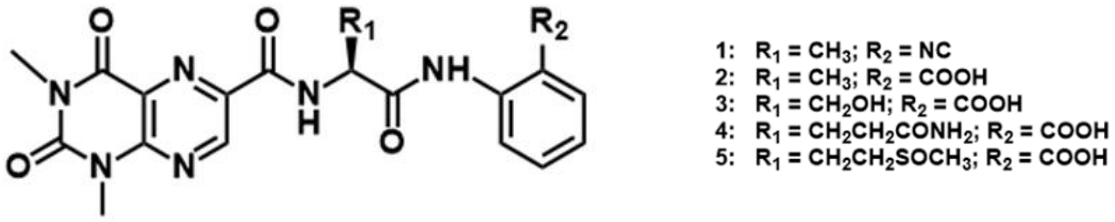

Figure 3.1.3. Target lumazine peptide analogues.

3.2. Analogue Design and Methods

The analogue goals for this project were driven by the desire to explore the effects of isonitrile functionality on a compound's biological activity. As a result, our goals for the synthesis of these peptides required the synthesis of each of the previously discovered natural products coupled with an analogue in which R_2 was replaced with an isonitrile group. By synthesizing the natural products and an isonitrile equivalent, we hope to compare the activity of these analogues to better assess the biological effects of this functional group. Given that the natural products exist as tripeptides, this provided convenient disconnections in the molecule consisting of three fragments. These natural disconnections are advantageous in providing a

modular approach to the synthesis for the creation of a variety of different analogues beyond those shown here using commercially available reagents. For example, a variety of amino acids can be used to create a new lumazine acid peptide analogue with minimal modification of synthetic methods.

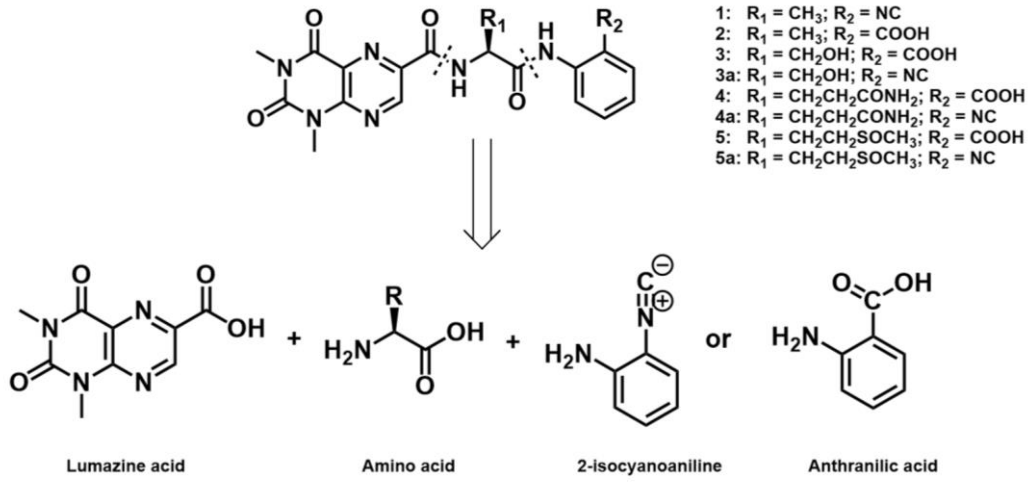

Figure 3.2.1. Target lumazine peptide analogues and fragments with key disconnections.

A synthesis of similar peptides was reported in 2017 by Penjarla et al., but attempts at this method proved unreliable, and thus required a new approach to the synthesis of the lumazine acid. Our early efforts at synthesizing the lumazine acid fragment began with a diazotization of 1,3-dimethyl-aminouracil using sodium nitrite and aniline to form 6-amino1,3-dimethyl-5-phenylazo-uracil, which was then reacted with diethyl acetylene dicarboxylate in DMF at 150°C. Previously published routes towards the synthesis of the desired lumazine acid reported in 1981 and 2017 used dimethylacetylene dicarboxylate or diethylacetylene dicarboxylate achieve a diester product, followed by tandem acid hydrolysis –

monodecarboxylation to achieve the lumazine carboxylic acid product.[23] However, our attempts at these methods yielded a dicarboxylic acid product, which led us to try a new synthetic route.

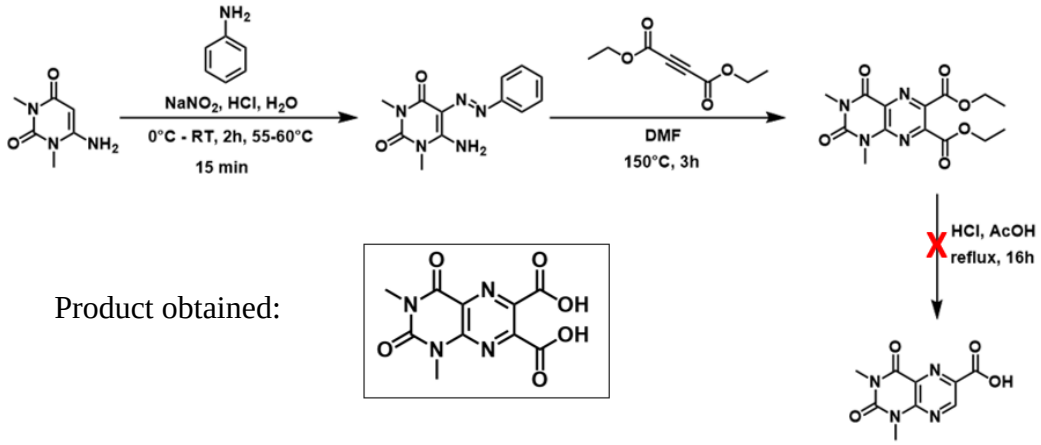

Scheme 3.2.2. Attempt at published route towards lumazine acid.

In our next attempt to synthesis the desired lumazine acid, we began once again with a diazotization of 1,3-dimethyl-aminouracil using sodium nitrite and aniline to form 6-amino1,3-dimethyl-5-phenylazo-uracil. In order to avoid producing a diester product, and thus the dicarboxylic acid product obtained in our last route, we instead reacted 6-amino1,3-dimethyl-5-phenylazo-uracil with methyl propiolate. We were able to obtain a cyclized ester product, but had difficulty in removing the aniline installed by our diazotization step. When we attempted to hydrolyze the ester product, the reaction suffered from poor yield and gave numerous side products. In an attempt to access the lumazine acid product directly from 6-amino1,3-dimethyl-5-phenylazo-uracil, we attempted a reaction with propiolic acid, but were unsuccessful in obtaining our desired product.

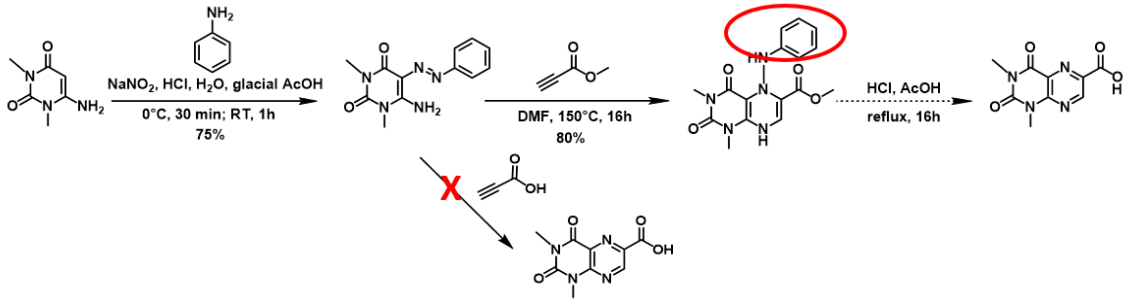

Scheme 3.2.3. Additional attempted routes in the synthesis of a lumazine acid.

In our recent and most successful route in the synthesis of the lumazine acid fragment of the peptide, we began with a nitrosation of 6-amino-1,3-dimethyluracil using sodium nitrite and aqueous acetic acid.[24] The resulting product was then reacted with methyl propiolate and heated to reflux to yield a cyclized lumazine methyl ester compound, which was then refluxed in hydrochloric acid to yield the lumazine acid portion of the peptide.

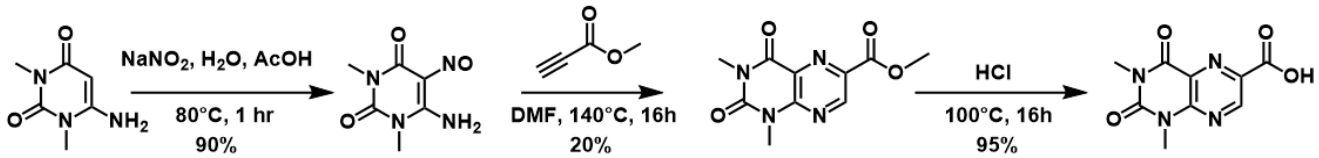

Scheme 3.2.4. Synthetic route towards the production of a lumazine acid.

For the synthesis of 2-isocyanoaniline, we began by performing a benzyl protection of benzene 1,2-diamine using potassium carbonate and benzyl bromide to achieve a mono-protected product, which was then reacted with two equivalents of potassium carbonate and sodium 2-chloro-2,2-difluoroacetate to obtain N-benzyl-2-isocyanoaniline.[25] Finally, we intend to

deprotect the N-benzyl-2-isocyanoaniline by performing a palladium on carbon hydrogenation to obtain the desired product, 2-isocyanoaniline.

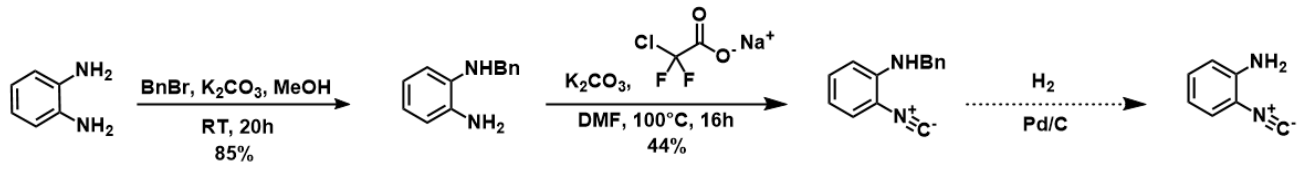

Scheme 3.2.5. Synthetic route towards 2-isocyanoaniline.

For our first peptide coupling to methyl L-alanine hydrochloride, the lumazine acid was reacted using DIPEA as a base to deprotonate the nitrogen of methyl L-alanite hydrochloride and HATU to activate the acid. The dipeptide was then hydrolyzed under basic conditions using lithium hydroxide to yield the carboxylic acid product, (1,3-dimethyl-2,4-dioxo-1,2,3,4-tetrahydropteridine-6-carbonyl)-L-alanine.

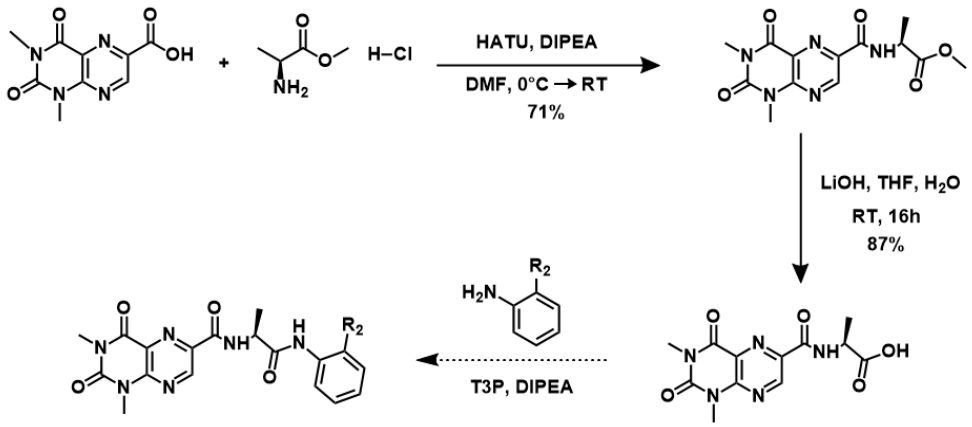

Scheme 3.2.6. Current route towards the synthesis of lumazine peptides.

3.3. Future Directions

Going forward, we will work to complete the deprotection N-benzyl-2-isocyanoanaline to achieve the desired isonitrile fragment, 2-isocyanoaniline, which will then undergo a final peptide coupling to achieve one of our target peptide products. Using this route, we will then be able to produce several analogues of the lumazine peptide natural products with isonitrile functionality. Upon the completion of our synthesis, we then intend to test the MICs of our compounds against a general panel of bacteria, including *Pseudomonas aeruginosa*, methicillin-susceptible *Staphylococcus aureus*, methicillin-resistant *Staphylococcus aureus*, *Escherichia coli*, *Acinetobacter baumannii*, and *Enterococcus faecalis*. Finally, we will perform a fluorophore titration on our compounds to test for the ability to bind metals and gain information about the potential binding ratio of these molecules when installed with isonitrile functionality.

4. Experimental

4.1 Instrumentation and General Notes

NMR spectra were obtained using the following spectrometers: Bruker Avance III 600 (600/150 MHz), Varian INOVA 600 (600/150 MHz) or Varian INOVA 500 (500/125 MHz). Chemical shifts are in ppm relative to TMS and use the indicated solvent as an internal reference.

All non-aqueous reactions were performed in flame-dried glassware under an atmosphere of argon using HPLC-grade solvents dried by passage through activated alumina. Triethylamine (Et_3N) was freshly distilled over CaH prior to use. Dioxane was purchased from Alfa Aesar. Brine refers to a saturated aqueous solution of sodium chloride. "Column chromatography" refers to purification with a normal-phase gradient on a Biotage® flash chromatography purification system. All other chemicals were used as received from Oakwood, TCI America, Sigma-Aldrich, and Alfa Aesar**.**

4.2 Experimental Procedures for Tricepyridinium Bromide and Analogues

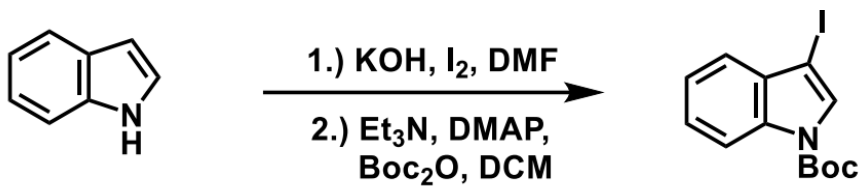

2 **94%** **3**

Tert-butyl 3-iodo-1H-indole-1-carboxylate S2. Indole **S1** (1.00 g, 8.54 mmol, 1.00 eq.) and potassium hydroxide (1.92 g, 34.2 mmol, 4.00 eq) were dissolved in dimethylformamide (15 mL). The solution was stirred for 20 minutes, then was cooled to 0°C. A solution of iodine (2.28 g, 8.97 mmol, 1.05 eq.)in dimethylformamide (15 mL) was then added dropwise to the reaction. The reaction was stirred for 15 minutes at 0°C then for 1 hour at room temperature. The organic

layer was extracted 3 times with dichloromethane and water. The combined organic layers were washed once with brine and then dried over anhydrous sodium sulfate, filtered, and concentrated under vacuum. The crude product was then dissolved in dichloromethane (30 mL). Dimethylaminopyridine (0.104 g, 0.854 mmol, 0.100 eq.) and freshly distilled triethylamine (3.57 mL, 25.6 mmol, 3.00 eq.) were added to the solution followed by di-tert-butyl dicarbonate (2.05 g, 9.39 mmol, 1.10 eq). The reaction stirred at room temperature for two hours. The organic layer was extracted 3 times with dichloromethane and water. The organic layers were combined and washed once with brine and then dried over anhydrous sodium sulfate, filtered, and concentrated under vacuum. The product was then purified using silica column chromatography (0-10% ethyl acetate in hexanes) yielding the title compound as a colorless oil (2.77 g, 94% yield.) **^{1}H NMR** (600 MHz, $CDCl_3$) δ 8.15 (m, 1H), 7.76 (br s, 1H), 7.42 (d, J = 7.7 Hz, 1H), 7.39 (t, J = 7.7 Hz, 1H), 7.33 (t, J = 7.5 Hz, 1H), 1.69 (s, 9H). **^{13}C NMR** (125 MHz, $CDCl_3$) δ 148.78, 134.94, 132.18, 130.17, 125.44, 123.42, 121.59, 115.16, 84.36, 65.58, 28.27. **HRMS** Accurate Mass (ES+): Found 343.00617 (-0.59 ppm), $C_{13}H_{14}O_2N^{127}I$ (M) requires 343.00637.1

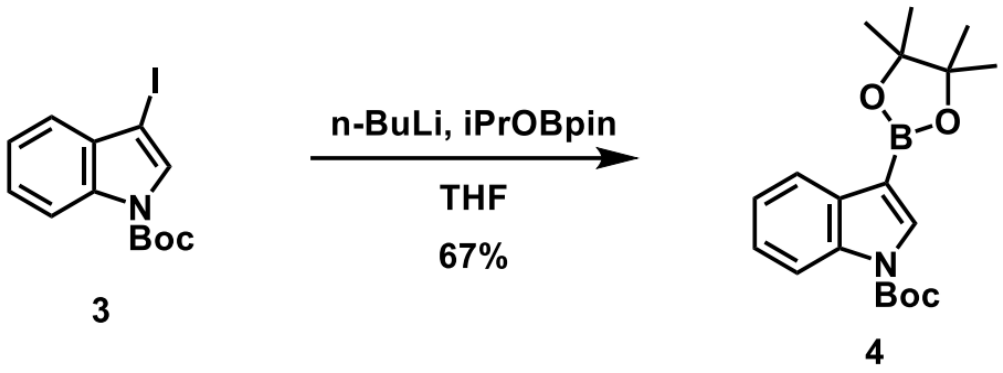

3 4

Tert-butyl 3-(4,4,5,5-tetramethyl-1,3,2-dioxaborolan-2-yl)-1H-indole-1-carboxylate S4. S3 (2.57 g, 7.50 mmol, 1.00 eq.) was dissolved in anhydrous tetrahydrofuran (30 mL) and cooled to -78°C. N-butyllithium (4.00 mL, 8.25 mmol, 1.10 eq.) was added to the solution dropwise. The reaction was stirred for 30 minutes at -78°C. 2-Isopropoxy-4,4,5,5-tetramethyl-1,3,2-dioxaborolane (1.68 mL, 8.25 mmol, 1.10 eq.) was then added dropwise to the reaction. The reaction stirred for 1 hour at -78°C, then at room temperature for an additional 30 minutes. 15 mL of saturated monopotassium phosphate solution was then added to the reaction flask. The organic layer was extracted with diethyl ether and water 3 times. The organic layers were combined and washed once with brine. The product was then dried over anhydrous sodium sulfate, filtered, and concentrated under vacuum. The product was purified using silica column chromatography (0-5% ethyl acetate in hexanes) yielding the title compound as a brown oil (1.26 g, 49% yield). **^{1}H NMR** (600 MHz, $CDCl_3$) δ 8.16 (d, J = 8.1 Hz, 1H), 8.01 (s, 1H), 7.98 (ddd, J = 7.7, 1.3, 0.7 Hz, 1H), 7.30 (ddd, J = 8.4, 7.3, 1.3 Hz, 1H), 7.28 – 7.24 (m, 3H), 1.66 (s, 9H), 1.38 (s, 12H). **^{13}C NMR** (150 MHz, CDCl3) δ 149.57, 136.28, 135.32, 133.63, 124.33, 123.05, 122.75, 115.04, 83.99, 83.49, 28.34, 25.05. **HRMS** Accurate Mass (ES+): Found 343.20610 (-0.87 ppm), $C_{19}H_{27}O_4N^{10}B$ (M + H+) requires 343.20640.

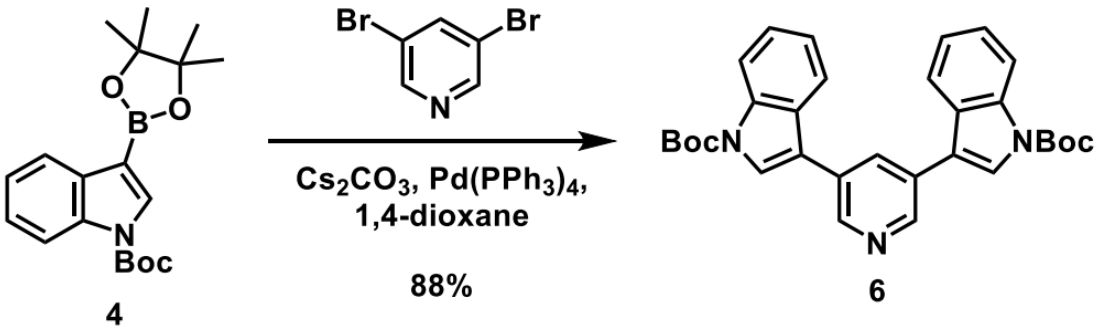

Di-tert-butyl 3,3'-(pyridine-3,5-diyl)bis(1H-indole-1-carboxylate) S6.

Tetrakis(triphenylphosphine)palladium(0) (0.141 g, 0.100 eq.) was dissolved in 1,4 dioxane (12.5 mL) and left to stir at room temperature for 20 minutes, resulting in a black solution. Cesium carbonate (1.99 g, 5.00 eq.), **S5** (1.26 g, 3.00 eq.) dissolved in 1,4 dioxane, (12.5 mL) and 3,5 dibromopyridine (0.298 g, 1.22 mmol, 1.00 eq) were added to the solution. The reaction was heated to reflux and stirred for 18 hours. The organic layer was extracted 3 times using dichloromethane and washed once with water. The organic layers were combined and washed with brine once, then dried over anhydrous sodium sulfate, filtered, and concentrated under vacuum. The product was purified using silica column chromatography (0-40% ethyl acetate in hexanes) to afford the title compound as a light brown solid (549.1 mg, 88% yield). **^{1}H NMR** (500 MHz, $CDCl_3$) δ 8.92 (d, J = 2.1 Hz, 2H), 8.31 – 8.27 (m, 2H), 8.26 (br s, 1H), 7.87 (s, 2H), 7.82 (dt, J = 7.9, 0.9 Hz, 2H), 7.43 (ddd, J = 8.4, 7.2, 1.2 Hz, 2H), 7.35 (ddd, J = 8.1, 7.3, 1.1 Hz, 2H), 1.72 (s, 18H). **^{13}C NMR** (150 MHz, CDCl3) δ 149.72, 147.54, 136.05, 134.17, 130.12, 128.70, 125.19, 123.79, 123.49, 119.64, 118.67, 115.82, 84.49, 28.37. **HRMS** Accurate Mass (ES+): Found 510.23806 (-1.32 ppm), $C_{31}H_{32}O_4N_3$ (M + H+) requires 510.23873.

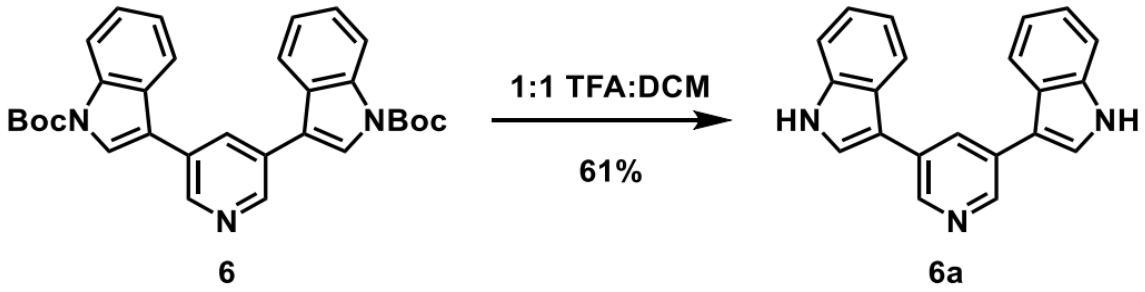

6 6a

3,5-di(1H-indol-3-yl)pyridine 6a. S6 (0.570 g, 1.120 mmol, 1 eq.) was dissolved in dichloromethane (2 mL) and cooled to 0 °C. Trifluoroacetic acid (2 mL) was added dropwise into the solution, and the reaction stirred at room temperature for 4 hours. The reaction was brought to pH 7 with 2M potassium hydroxide. The organic layer was extracted 4 times with ethyl acetate and washed once with brine. A buoyant white precipitate formed upon standing of the aqueous layer; this was collected via gravity filtration and combined with the organic layers. Combined organic layers were then dried over anhydrous sodium sulfate, filtered, and concentrated in vacuo. Crude product was dry-loaded onto a silica column and purified using silica column chromatography (50-100% ethyl acetate in hexanes, then 0-15% methanol in dichloromethane) affording a tan powder with low solubility in organic solvents, with the exception of pyridine (210 mg, 65% yield). **^{1}H NMR** (600 MHz, DMSO-d6) δ 11.55 (s, 2H), 8.81 (s, 2H), 8.29 (t, J = 1.9 Hz, 1H), 7.99 – 7.89 (m, 4H), 7.51 (d, J = 8.0 Hz, 2H), 7.20 (t, J = 7.3 Hz, 2H), 7.15 (t, J = 7.3 Hz, 2H). **^{13}C NMR** (150 MHz, DMSO-d6) δ 144.24, 136.95, 131.72, 130.64, 124.94, 124.44, 121.69, 120.01, 118.83, 112.37, 112.14. **HRMS** Accurate Mass (ES+): Found 510.23806 (-1.32 ppm), $C_{31}H_{32}O_4N_3$ requires 510.23873.

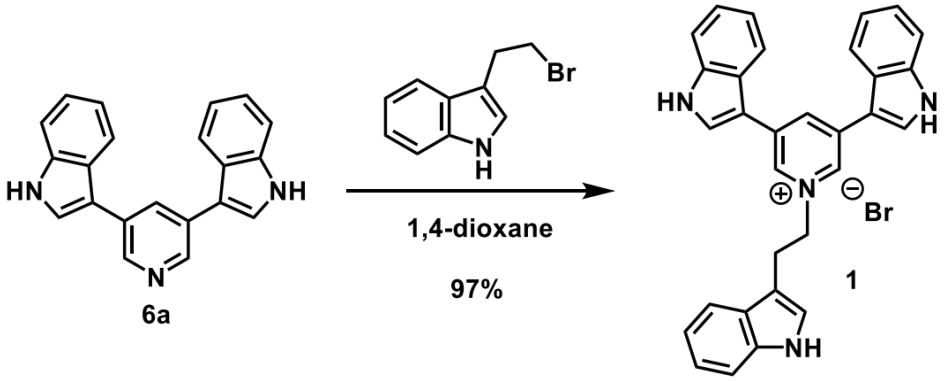

1-(2-(1H-indol-3-yl)ethyl)-3,5-di(1H-indol-3-yl)pyridin-1-ium bromide 1. Disubstituted pyridine 6a (30 mg, 0.097 mmol, 1 eq.) was dissolved in 1,4-dioxane (1 mL) and 3-(2-bromoethyl)indole (32.6 mg, 0.145 mmol, 1.5 eq.) was added. The reaction mixture was heated to reflux and stirred for 72 hours. The reaction mixture was then cooled to room temperature and loaded directly onto a short silica column, which was flushed first with 100% ethyl acetate to elute trace starting materials, followed by 100% methanol. The ethyl acetate fraction was concentrated in vacuo, then reloaded onto the column and flushed again with 100% ethyl acetate, then 100% methanol. The methanol fractions were combined and concentrated in vacuo to furnish the title compound as a yellow powder (50 mg, 97% yield). **^{1}H NMR** (600 MHz, CD_3OD) δ 8.65 (t, J = 1.6 Hz, 1H), 8.37 (d, J = 1.7 Hz, 2H), 7.68 (s, 2H), 7.50 (d, J = 7.9 Hz, 1H), 7.46 (d, J = 8.2 Hz, 2H), 7.36 (d, J = 8.0 Hz, 3H), 7.20 (ddd, J = 8.1, 7.1, 1.0 Hz, 2H), 7.16-7.10 (m, 3H), 7.04 (ddd, J = 8.0, 7.1, 0.9 Hz, 1H), 6.99 (s, 1H), 4.91 (t, J = 6.1 Hz, 2H), 3.52 (t, J = 6.1 Hz, 2H). **^{13}C NMR** (150 MHz, CD_3OD) δ 138.75, 138.35, 138.25, 137.41, 137.00, 128.00, 127.37, 125.44, 125.31, 123.83, 123.15, 122.36, 120.59, 119.29, 118.72, 113.34, 113.02, 110.58, 109.70, 63.78, 28.68. **HRMS** Accurate Mass (ES): Found 453.20631 (-2.34 ppm), $C_{31}H_{25}N_4$ + (M) requires 453.20737.

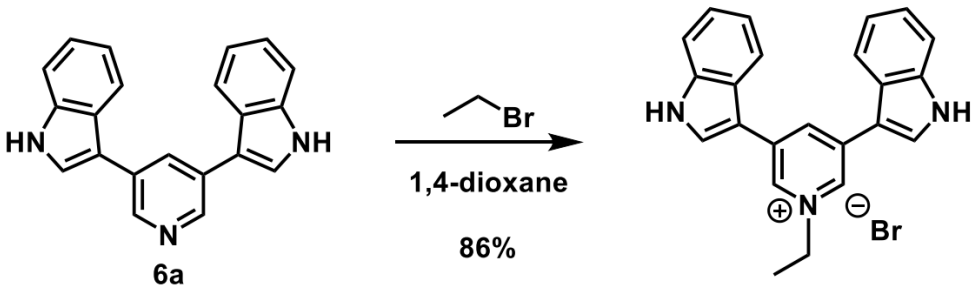

1-ethyl-3,5-di(1H-indol-3-yl)pyridin-1-ium 7. Disubstituted pyridine 6a (20 mg, 0.0646 mmol, 1 eq.) was dissolved in 1,4-dioxane (1 mL) and 1-bromoethane (7.2 µL, 0.0970 mmol, 1.5 eq.) was added. The reaction mixture was covered with aluminum foil, heated to reflux, and stirred for 48 hours. Additional 1-bromoethane (7.2 µL, 0.0970 mmol, 1.5 eq.) was added and the reaction continued to stir at reflux for an additional 24 hours. The reaction mixture was then cooled to room temperature and loaded directly onto a short silica column, which was flushed first with 100% ethyl acetate to elute trace starting materials, followed by 100% methanol containing 1% acetic acid. The ethyl acetate fraction was concentrated in vacuo, then reloaded onto the column and flushed again with 100% ethyl acetate, then 100% methanol containing 1% acetic acid. The methanol fractions were combined and concentrated in vacuo to furnish the title compound as a yellow powder (23.2 mg, 86% yield). **^{1}H NMR** (600 MHz, CD_3OD) δ 9.03 – 8.98 (m, 2H), 8.95 (s, 1H), 8.03 (s, 2H), 8.00 (dd, J = 6.4, 2.1 Hz, 2H), 7.55 (dd, J = 6.5, 2.0 Hz, 2H), 7.31 – 7.24 (m, 4H), 4.78 (q, J = 7.3 Hz, 2H), 1.78 (t, J = 7.3 Hz, 3H). **^{13}C NMR** (150 MHz, CD_3OD) δ 139.17, 139.01, 137.54, 137.47, 127.63, 125.79, 123.95, 122.40, 119.41, 113.58, 110.82, 58.68, 24.20. **HRMS** Accurate Mass (ES): Found 338.1645 (-1.99 ppm), $C_{23}H_{20}N_3$ + (M) requires 338.16517.

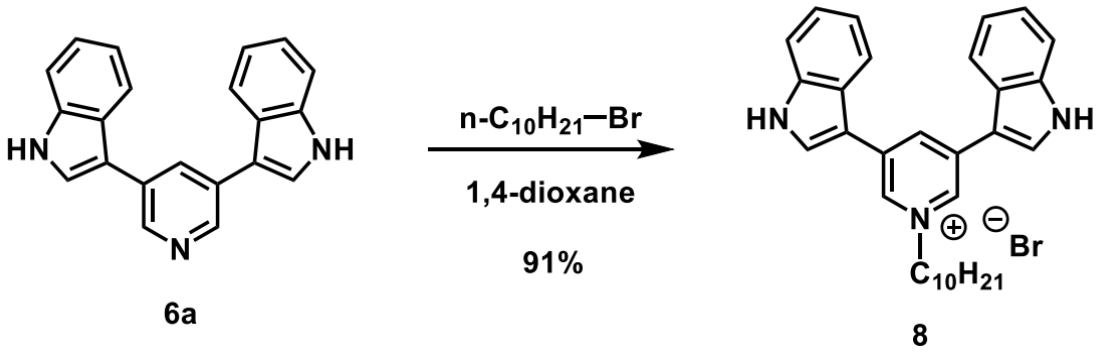

1-decyl-3,5-di(1H-indol-3-yl)pyridin-1-ium 8. Disubstituted pyridine 6a (30 mg, 0.097 mmol, 1 eq.) was dissolved in 1,4-dioxane (1 mL) and 1-bromodecane (30 µL, 0.145 mmol, 1.5 eq.) was added. The reaction mixture was heated to reflux and stirred for 72 hours. The reaction mixture was then cooled to room temperature and loaded directly onto a short silica column, which was flushed first with 100% ethyl acetate to elute trace starting materials, followed by 100% methanol. The ethyl acetate fraction was concentrated in vacuo, then reloaded onto the column and flushed again with 100% ethyl acetate, then 100% methanol. The methanol fractions were combined and concentrated in vacuo to furnish the title compound as a yellow powder (46.7 mg, 91% yield). **^{1}H NMR** (600 MHz, CD_3OD) δ 8.80 (s, 2H), 8.64 (s, 1H), 7.95 (s, 2H), 7.86 (dd, J = 6.8, 1.7 Hz, 2H), 7.47 (d, J = 7.5 Hz, 2H), 7.23-7.15 (m, 4H), 4.59 (t, J = 7.5 Hz, 2H), 2.03 (p, J = 7.3 Hz, 2H), 1.44 (p, J = 7.5, 7.1 Hz, 2H), 1.38 (p, J = 6.5 Hz, 2H), 1.27-1.19 (m, 10H), 0.83 (t, J = 7.1 Hz, 3H). **^{13}C NMR** (150 MHz, CD_3OD) δ 138.83, 138.65, 137.15, 136.51, 127.75, 125.55, 123.92, 122.40, 119.44, 113.57, 110.57, 63.09, 32.98, 32.82, 30.73, 30.54, 30.37, 30.10, 27.28, 23.66, 14.41. **HRMS** Accurate Mass (ES): Found 450.28929 (-2.41 ppm), $C_{31}H_{36}N_3$ + (M) requires 450.29037.

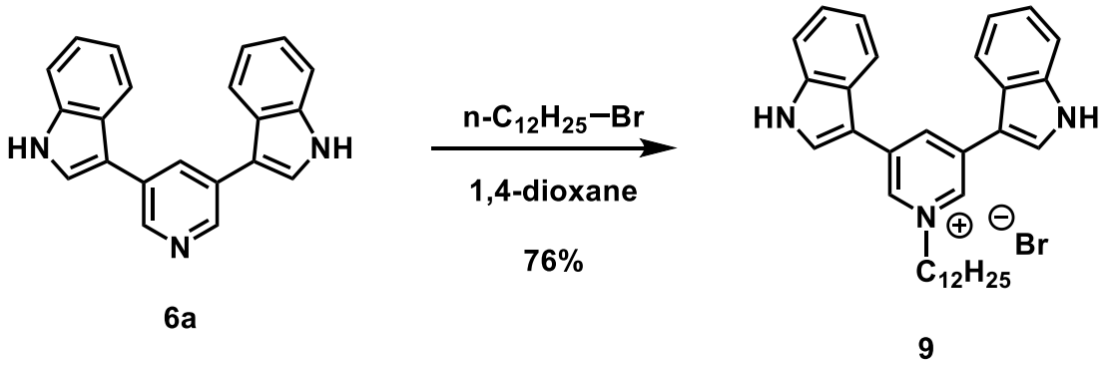

6a 9

1-dodecyl-3,5-di(1H-indol-3-yl)pyridin-1-ium 9. Disubstituted pyridine 6a (20 mg, 0.0646 mmol, 1 eq.) was dissolved in 1,4-dioxane (1 mL) and 1-bromododecane (23.3 µL, 0.0970 mmol, 1.5 eq.) was added. The reaction mixture was heated to reflux and stirred for 72 hours. The reaction mixture was then cooled to room temperature and loaded directly onto a short silica column, which was flushed first with 100% ethyl acetate to elute trace starting materials, followed by 100% methanol. The ethyl acetate fraction was concentrated in vacuo, then reloaded onto the column and flushed again with 100% ethyl acetate, then 100% methanol. The methanol fractions were combined and concentrated in vacuo to furnish the title compound as a yellow powder (27.2 mg, 76% yield). **^{1}H NMR** (600 MHz, $CD^{3}OD$) δ 8.98 (s, 2H), 8.93 (s, 1H), 8.03 (s, 2H), 7.99 (dd, J = 6.6, 1.7 Hz, 2H), 7.54 (dd, J = 6.7, 1.8 Hz, 2H), 7.31 – 7.24 (m, 4H), 4.72 (t, J = 7.5 Hz, 2H), 2.15 (p, 7.6 Hz, 2H), 1.51 (p, J = 7.0 Hz, 2H), 1.44 (p, 6.7 Hz, 2H), 1.38-1.19 (m, 16H), 0.87 (t, J = 7.1 Hz, 3H). **^{13}C NMR** (150 MHz, CD_3OD) δ 139.04, 138.99, 137.71, 137.49, 127.63, 125.75, 124.01, 122.44, 119.42, 113.56, 110.80, 63.20, 33.02, 32.76, 30.71, 30.58, 30.52, 30.42, 30.09, 27.30, 24.11, 23.69, 14.41. **HRMS** Accurate Mass (ES): Found 478.32117 (-1.06 ppm), $C_{33}H_{40}N_3$ + (M) requires 478.32167.

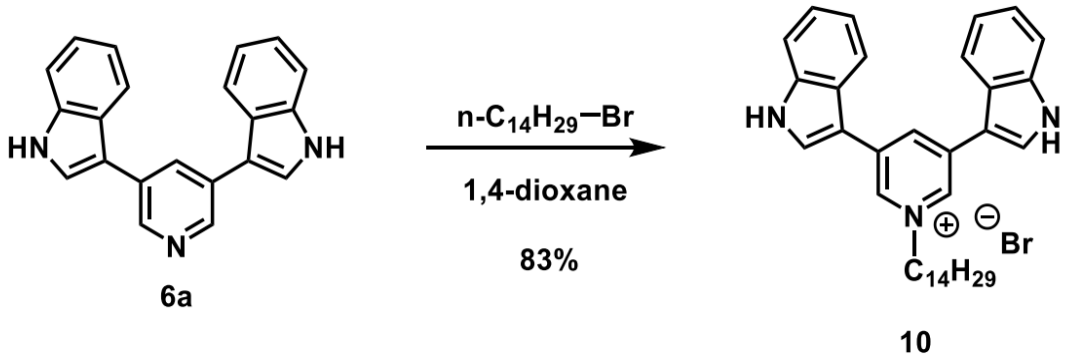

6a

10

3,5-di(1H-indol-3-yl)-1-tetradecylpyridin-1-ium 10. Disubstituted pyridine 6a (20 mg, 0.0676 mmol, 1 eq.) was dissolved in 1,4-dioxane (1 mL) and 1-bromotetradecane (28.8 µL, 0.0970 mmol, 1.5 eq.) was added. The reaction mixture was heated to reflux and stirred for 72 hours. The reaction mixture was then cooled to room temperature and loaded directly onto a short silica column, which was flushed first with 100% ethyl acetate to elute trace starting materials, followed by 100% methanol. The ethyl acetate fraction was concentrated in vacuo, then reloaded onto the S8 column and flushed again with 100% ethyl acetate, then 100% methanol. The methanol fractions were combined and concentrated in vacuo to furnish the title compound as a yellow powder (31.2 mg, 83% yield). **^{1}H NMR** (600 MHz, CD_3OD) δ 8.91 (s, 2H), 8.82 (s, 1H), 8.00 (s, 2H), 7.94 (dd, J = 6.6, 1.8 Hz, 2H), 7.52 (dd, J = 6.7, 1.8 Hz, 2H), 7.28 – 7.20 (m, 4H), 4.67 (t, J = 7.5 Hz, 2H), 2.10 (p, J = 7.6 Hz, 2H), 1.48 (p, 7.0 Hz, 2H), 1.42 (p, 6.8 Hz, 2H), 1.36 – 1.18 (m, 23H), 0.87 (t, J = 7.1 Hz, 4H). **^{13}C NMR** (150 MHz, CD_3OD) δ 138.94, 138.91, 137.49, 137.09, 127.70, 125.68, 123.97, 122.42, 119.43, 113.58, 110.70, 63.16, 33.03, 32.77, 30.73, 30.70, 30.68, 30.56, 30.51, 30.42, 30.08, 27.27, 24.19, 23.70, 14.43. **HRMS** Accurate Mass (ES): Found 506.35261 (-0.73 ppm), $C_{35}H_{44}N_3$ + (M) requires 506.35297.

4.3. Biological Testing

Bacterial strains and culture conditions: Bacterial strains were generous gifts from Prof. Buttaro (Temple University). With the exception of UA159, cultures were grown from freezer stocks overnight (16-24 hr) with shaking at 37 °C in 10 mL media (Mueller-Hinton media for SH1000, OG1RF, MC4100, and PAO1, Todd Hewitt Broth for USA300-0114 and ATCC 33591). Bacterial cultures of UA159 were grown from a freshlystreaked Petri dish (grown from a freezer stock) overnight (16 hours) statically at 37 °C in a CO_2 incubator (5% CO_2) in 10 mL media (Tryptic Soy Broth containing 5% sucrose to reflect physiological conditions and promote biofilm formation). Growth curves were obtained for all bacterial strains by previous members of the group to determine the optical density (OD) of each strain in exponential growth; OD readings at a wavelength of 595 nm were taken every 10 minutes for 6 hours in a plate reader at 37 °C with shaking and repeated six times. This data was used without alteration for this report.

Hemolysis assay: Compounds were serially diluted in sterile DI water from a stock solution (1 mM in 10% DMSO/90% H2O) to yield twelve test concentrations. Defibrinated sheep's blood (Hemostat, DSB030, 1.5 mL) was centrifuged at 10,000 rpm for ten minutes. The supernatant was removed and the blood was resuspended in 1 mL of phosphate buffered saline (PBS). The centrifugation, supernatant removal, and resuspension was repeated three times until the supernatant was clear. The final cell suspension was diluted 1:20 with PBS and aliquoted into the microcentrifuge tubes containing the serially-diluted compounds. Tubes were then incubated at 37 °C for 1 hour with shaking at 200 rpm. Samples were then centrifuged at 10,000 rpm for ten minutes. The supernatant of each sample was carefully transferred to a flat-bottom 96-well plate

(Corning 3370), and absorbance measurements were taken at 540 nm using a plate reader. LC20 values were calculated by taking 20% of the difference between the absorbance values of the positive control (TritonX, 1% by volume, 100% lysis marker) and the negative control (sterile PBS, 0% lysis marker) and using that as a cutoff point. Assay was performed in triplicate to ensure reproducibility.

TRIAL 1	250 µM	125 µM	64 µM	32 µM	16 µM	8 µM	4 µM	2 µM	1 µM	0.5 µM	0.25 µM	0.125 µM
PBS buffer	0.0398	0.0512	0.0487	0.0499	0.0512	0.032	0.0472	0.0486	0.0415	0.0429	0.0443	0.0443
Triton X	0.3677	0.4131	0.7373	0.6971	0.056	0.032	0.0433	0.0437	0.0429	0.0436	0.0446	0.0462
S-7	0.3716	0.1188	0.0549	0.0512	0.05	0.0604	0.0472	0.0468	0.043	0.0414	0.045	0.043
S-8	0.364	0.2074	0.086	0.0683	0.0519	0.0518	0.0504	0.0464	0.0465	0.0432	0.0441	0.044
S-9	0.3261	0.1424	0.0683	0.0514	0.0489	0.0585	0.0458	0.0455	0.0436	0.0399	0.045	0.0438
S-10	0.3862	0.1482	0.0673	0.0537	0.0471	0.0489	0.0443	0.0447	0.0412	0.0343	0.0443	0.0452
S-1	0.3826	0.2132	0.0669	0.0542	0.0492	0.0523	0.0503	0.046	0.0447	0.0391	0.0462	0.0444

TRIAL 2	250 µM	125 µM	64 µM	32 µM	16 µM	8 µM	4 µM	2 µM	1 µM	0.5 µM	0.25 µM	0.125 µM
PBS buffer	0.0405	0.058	0.0444	0.0484	0.0512	0.0483	0.0356	0.0488	0.0531	0.0556	0.0565	0.0516
Triton X	1.0977	1.6338	0.5305	0.0884	0.0466	0.0405	0.0323	0.0467	0.0485	0.0484	0.046	0.0506
S-7	0.4661	0.0744	0.0513	0.05	0.0475	0.0614	0.0547	0.0499	0.0513	0.0501	0.0498	0.0603
S-8	0.5319	0.2851	0.0991	0.0669	0.0489	0.0523	0.0474	0.0489	0.0481	0.0517	0.0514	0.0604
S-9	0.5099	0.1716	0.0626	0.0519	0.0469	0.0524	0.0564	0.0561	0.0542	0.054	0.0552	0.0554
S-10	0.466	0.1924	0.0704	0.0489	0.0463	0.0502	0.0472	0.048	0.0485	0.0499	0.0517	0.0598
S-1	0.5265	0.2732	0.0763	0.0472	0.048	0.0524	0.0544	0.0494	0.0483	0.0508	0.0552	0.0686

TRIAL 3	250 µM	125 µM	64 µM	32 µM	16 µM	8 µM	4 µM	2 µM	1 µM	0.5 µM	0.25 µM	0.125 µM
PBS buffer	0.0437	0.0456	0.0536	0.0706	0.0558	0.0439	0.0529	0.0326	0.0429	0.0454	0.0453	0.0412
Triton X	1.6319	0.98	0.3139	0.0567	0.0488	0.0432	0.0449	0.0481	0.0445	0.0473	0.052	0.0483
S-7	0.5265	0.1268	0.0512	0.0435	0.0446	0.0432	0.0341	0.0498	0.0477	0.0504	0.055	0.046
S-8	0.5469	0.2365	0.1045	0.0686	0.0487	0.0494	0.0528	0.0471	0.0476	0.0486	0.0514	0.0476
S-9	0.4617	0.1601	0.0818	0.0485	0.0485	0.048	0.0494	0.0515	0.0482	0.0516	0.0534	0.0484
S-10	0.5909	0.1718	0.0736	0.0571	0.0495	0.0494	0.0504	0.0472	0.0471	0.0487	0.0492	0.0484
S-1	0.5867	0.2356	0.0842	0.051	0.0491	0.0496	0.051	0.0487	0.0478	0.0495	0.0491	0.0469

Table 4.3.1. Hemolysis data for all compounds tested, with optical densities at LD20 highlighted in red for each compound.

MIC Assay: Compounds were serially diluted in sterile DI water from a stock solution (1 mM in 10% DMSO/90% H2O) to yield twelve test concentrations. Overnight cultures were diluted 1:100 in 5 mL of the sterile media indicated above and grown with shaking at 37 °C to an optical

density (OD) reflecting exponential growth (with the exception of UA159, which was grown statically in a CO_2 incubator as described above). Bacteria were diluted to an optical density of 0.004 using the following equation: (x μL bacterial culture)(OD reading) = (0.004)(volume needed) and 100 μL was inoculated into each well of a flat-bottom 96-well plate (Corning 3370) containing 100 μL of compound solution. Plates were incubated statically at 37 °C for 72 hours (with the exception of UA159 plates, which were incubated in a CO_2 incubator statically for 24 hours), upon which time the MICs were scored visually. Compounds were tested in triplicate from separate cultures to ensure reproducibility.

4.4. Experimental Procedures for Lumazine Peptides

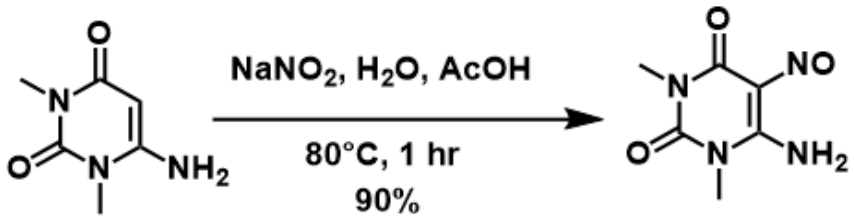

6-amino-1,3-dimethyl-5-nitrosopyrimidine-2,4(1H,3H)-dione. 6-amino-1,3-dimethyl uracil was dissolved in a 1:1 mixture of acetic acid and water (80 mL). Sodium nitrite (4 g, 60 mmol, 2 eq.) was dissolved in a small amount of water and added to the reaction dropwise with stirring. The reaction was heated to 80°C and left to stir for one hour. The reaction was then cooled at 0°C for 30 minutes. The reaction was then filtered and washed with cold water to give a bright pink solid filtrate as the title compound with no further purification (5.54 g, 90% yield). **^{1}H NMR** (600 MHz, CD_3OD) δ 5.49 (s, 2H), 3.42 (s, 3H), 3.39 (s, 3H).

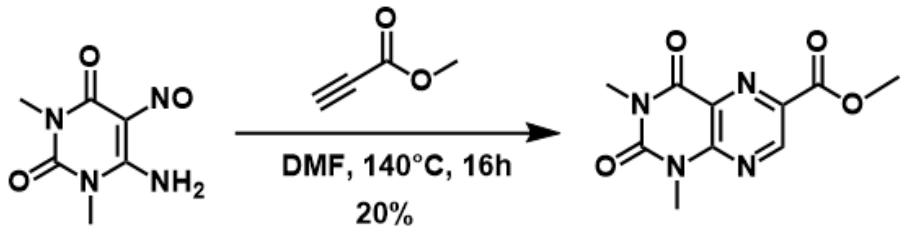

Methyl 1,3-dimethyl-2,4-dioxo-1,2,3,4-tetrahydropteridine-6-carboxylate. 6-amino-1,3-dimethyl-5-nitrosopyrimidine-2,4(1H,3H)-dione was dissolved in DMF (15 mL) at room temperature. Methyl propiolate (218 mg, 2.6 mmol, 1.1 eq.) was added to the reaction flask. The reaction flask was fitted with a reflux condenser and left to stir for 16 hours at 150°C. The reaction mixture was then washed 5 times with brine, and the organic layer was then extracted 3 times with DCM. The organic layer was dried over anhydrous sodium sulfate, filtered, and concentrated under vacuum. The crude mixture was then purified using silica column chromatography (25-80% ethyl acetate in hexanes) to afford a yellow powder (118 mg, 20% yield). **^{1}H NMR** (600 MHz, $CDCl_3$) δ 9.34 (s, 1H), 4.05 (s, 3H), 3.76 (s, 3H), 3.56 (s, 3H). **^{13}C NMR** (150 MHz, $CDCl_3$) δ 163.83, 159.05, 150.46, 149.71, 149.35, 138.83, 126.88, 53.34, 29.97, 29.37.

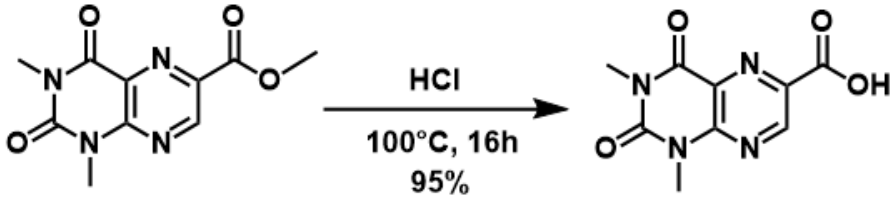

1,3-dimethyl-2,4-dioxo-1,2,3,4-tetrahydropteridine-6-carboxylic acid. Methyl 1,3-dimethyl-2,4-dioxo-1,2,3,4-tetrahydropteridine-6-carboxylate (114 mg, 0.457 mmol)was dissolved in excess HCl (3 mL). The reaction was fitted with a reflux condenser, heated to 100°C, and left to stir for 16 hours. The reaction mixture was concentrated under vacuum to yield the final product as a brown powder with any further purification (103 mg, 95% yield). **^{1}H NMR** (600 MHz, D_2O) δ 9.26 (s, 1H), 3.73 (s, 3H), 3.51 (s, 3H). **^{13}C NMR** (150 MHz, D_2O) δ 169.72, 162.01, 151.90, 148.95, 148.38, 144.08, 126.21, 29.47, 28.81.

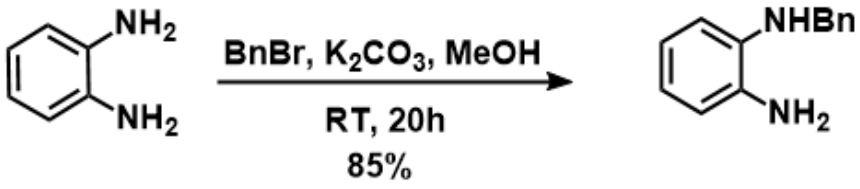

N-benzylbenzene-1,2-diamine. Benzene-1,2-diamine (2.11g, 19.5 mmol, 4.63 eq.) and potassium carbonate (1.60 g, 11.6 mmol, 2.75 eq.) were added to a reaction flask and dissolved in MeOH (7.5 mL). Benzyl bromide (0.50 mL, 4.21 mmol, 1 eq.) was added dropwise to reaction mixture with stirring. The reaction was left to stir at room temperature for 20 hours. The crude reaction mixture was concentrated under vacuum and then purified using silica column chromatography (10-75% ethyl acetate in hexanes) to yield a dark red oil (705 mg, 85% yield). **^{1}H NMR** (600 MHz, $CDCl_3$) δ 7.43 – 7.36 (m, 5H), 6.81 (m, 1H), 6.74 – 6.69 (m, 3H), 4.32 (s, 2H), 3.49 (s, 2H). **^{13}C NMR** (150 MHz, $CDCl_3$) δ 139.55, 137.87, 134.31, 128.75, 127.94, 127.41, 120.89, 118.97, 116.68, 112.12, 48.80.

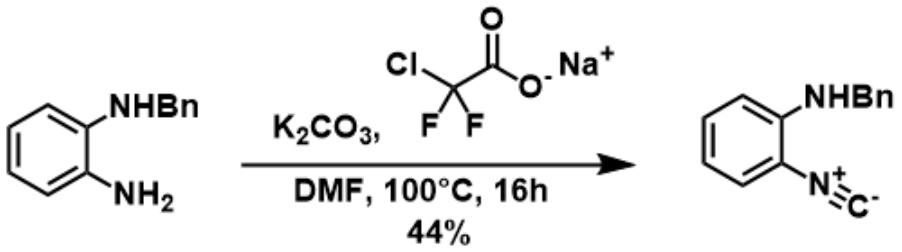

N-benzyl-2-isocyanoaniline. N-benzylbenzene-1,2-diamine (145 mg, 0.729 mmol), potassium carbonate (201 mg, 1.46 mmol, 2 eq.), and sodium-2-chloro-2,2-difluoroacetate (222 mg, 1.46 mmol, 2 eq.) were added to a reaction and dissolved in DMF (8.5 mL). The reaction was heated to 100°C and left to stir for 16 hours. The reaction mixture was then extracted 3 times with DCM. The combined organic layers were then washed with brine 5 times. The organic layer was dried over anhydrous sodium sulfate, filtered, and concentrated under vacuum. The final product was isolated using silica column chromatography (0-75% ethyl acetate in diethyl ether) to yield a light brown oil (67 mg, 44% yield). **^{1}H NMR** (600 MHz, $CDCl_3$) δ 7.96 (m, 1H), 7.82 (m, 1H), 7.33 (m, 5H), 7.29 (m, 1H), 7.18 (m, 1H), 5.27 (s, 2H), 4.88 (m, 1H). **^{13}C NMR** (150 MHz, $CDCl_3$) δ 163.57, 144.09, 143.35, 135.60, 129.19, 128.42, 127.23, 123.23, 122.42, 120.59, 110.16, 48.99.

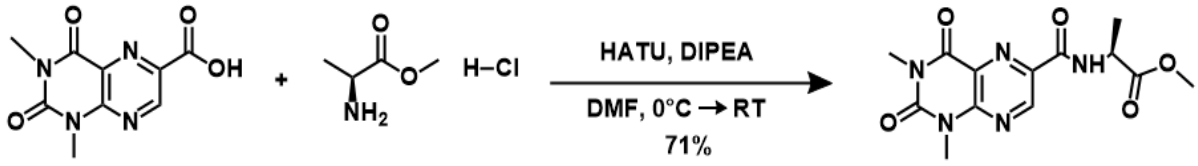

Methyl (1,3-dimethyl-2,4-dioxo-1,2,3,4-tetrahydropteridine-6-carbonyl)-L-alaninate. 1,3-Dimethyl-2,4-dioxo-1,2,3,4-tetrahydropteridine-6-carboxylic acid (103 mg, 0.426 mmol)was

dissolved in DMF (2 mL) and HATU (263 mg, 1.09 mmol, 2.5 eq.) was added and left to stir for 10 minutes at room temperature. In a separate reaction flask, methyl L-alaninate hydrochloride (67 mg, 0.48 mmol, 1.1 eq.) was dissolved in DMF (2 mL) and DIPEA (169 mg, 1.31 mmol, 3 eq.) was added, and the reaction was stirred at room temperature for 10 minutes. The reaction flask containing dimethyl-2,4-dioxo-1,2,3,4-tetrahydropteridine-6-carboxylic acid and HATU was then cooled to 0°C, and the mixture containing methyl L-alaninate hydrochloride and DIPEA was added dropwise. The reaction was brought to room temperature and left to stir for 16 hours. The reaction mixture was extracted 3 times with DCM. The organic layers were combined and washed once with brine. The organic layer was dried over anhydrous sodium sulfate, filtered, and concentrated under vacuum. The product was purified using silica column chromatography (70-100% ethyl acetate in hexanes) to afford a white solid (99 mg, 71% yield). **^{1}H NMR** (600 MHz, $CDCl_3$) δ 9.42 (s, 1H), 4.82 (q, 1H), 3.78 (s, 3H), 3.76 (s, 3H), 3.56 (s, 3H), 1.58 (d, 3H). **^{13}C NMR** (150 MHz, $CDCl_3$) δ 172.70, 161.89, 159.36, 150.46, 149.73, 148.04, 139.96, 125.29, 52.73, 48.44, 38.75, 30.00, 29.35, 18.16.

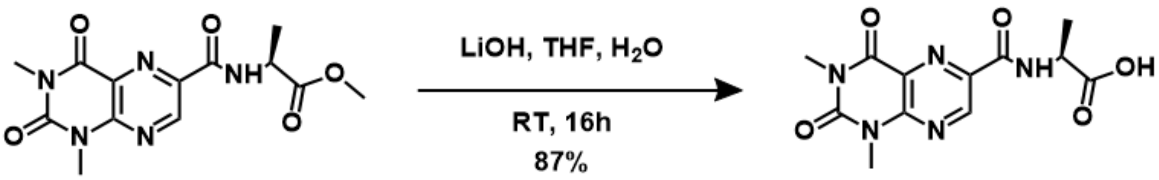

(1,3-dimethyl-2,4-dioxo-1,2,3,4-tetrahydropteridine-6-carbonyl)-L-alanine. Methyl (1,3-dimethyl-2,4-dioxo-1,2,3,4-tetrahydropteridine-6-carbonyl)-L-alaninate (27 mg, 0.084 mmol) was dissolved in THF (4 mL) with stirring. Lithium hydroxide (20 mg, 0.84 mmol, 10 eq.) was dissolved in H_2O (1 mL) and added dropwise to the reaction flask. The reaction was left to stir

overnight at room temperature. The organic layer was extracted with ethyl acetate and brought to a pH of 3. The organic layer was then extracted 3 times with ethyl acetate and washed once with brine. The organic layer was dried over anhydrous sodium sulfate, filtered, and concentrated under vacuum to yield a yellow solid as the final product (22.5 mg, 87% yield). **^{1}H NMR** (600 MHz, $CDCl_3$) δ 9.17 (s, 1H), 9.00 (s, 1H), 4.80, (q, 1H), 3.11 (s, 3H), 3.02 (s, 3H), 1.61 (d, 3H). **^{13}C NMR** (150 MHz, $CDCl_3$) δ 175.85, 171.32, 166.13, 163.86, 156.21, 147.45, 129.11, 124.27, 60.49, 29.74, 21.13, 14.23.

4.5. Spectral Data

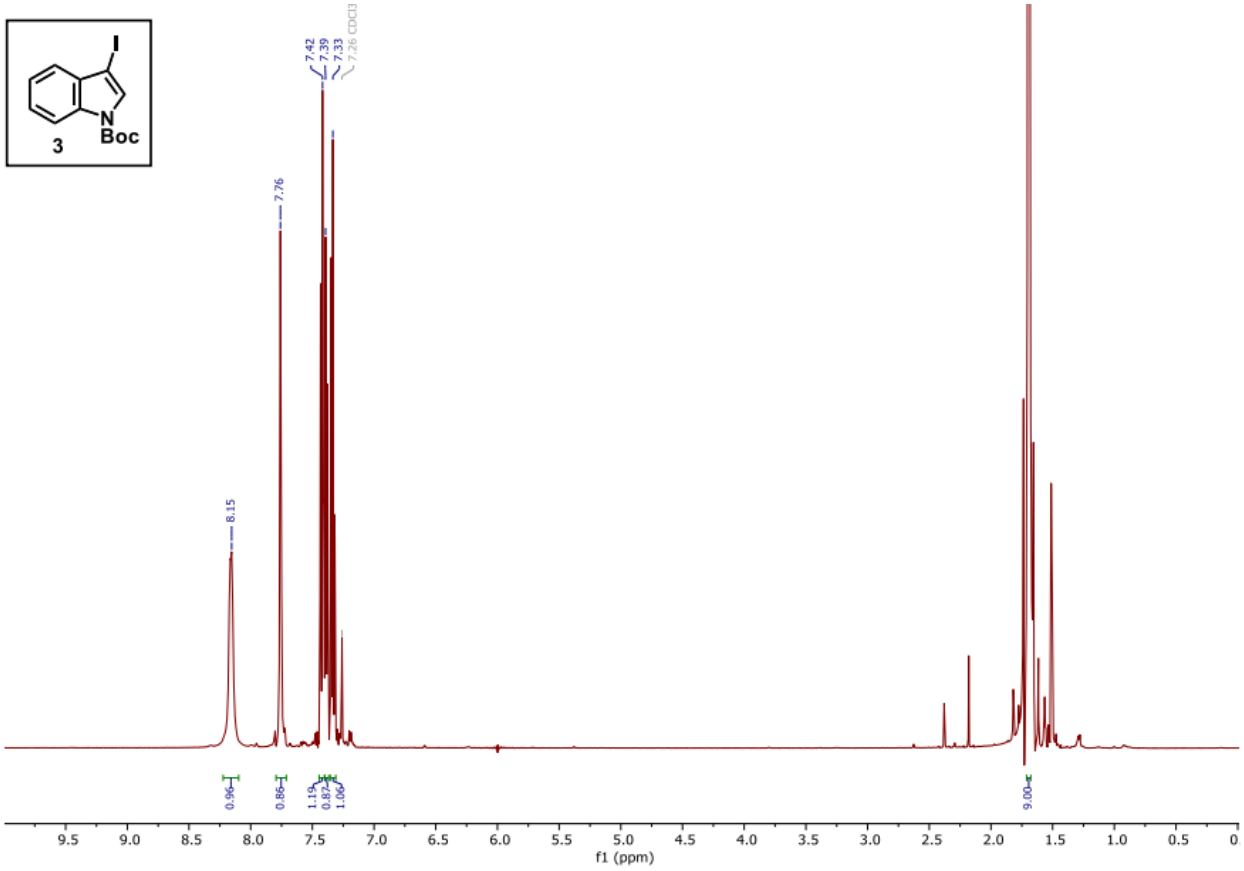

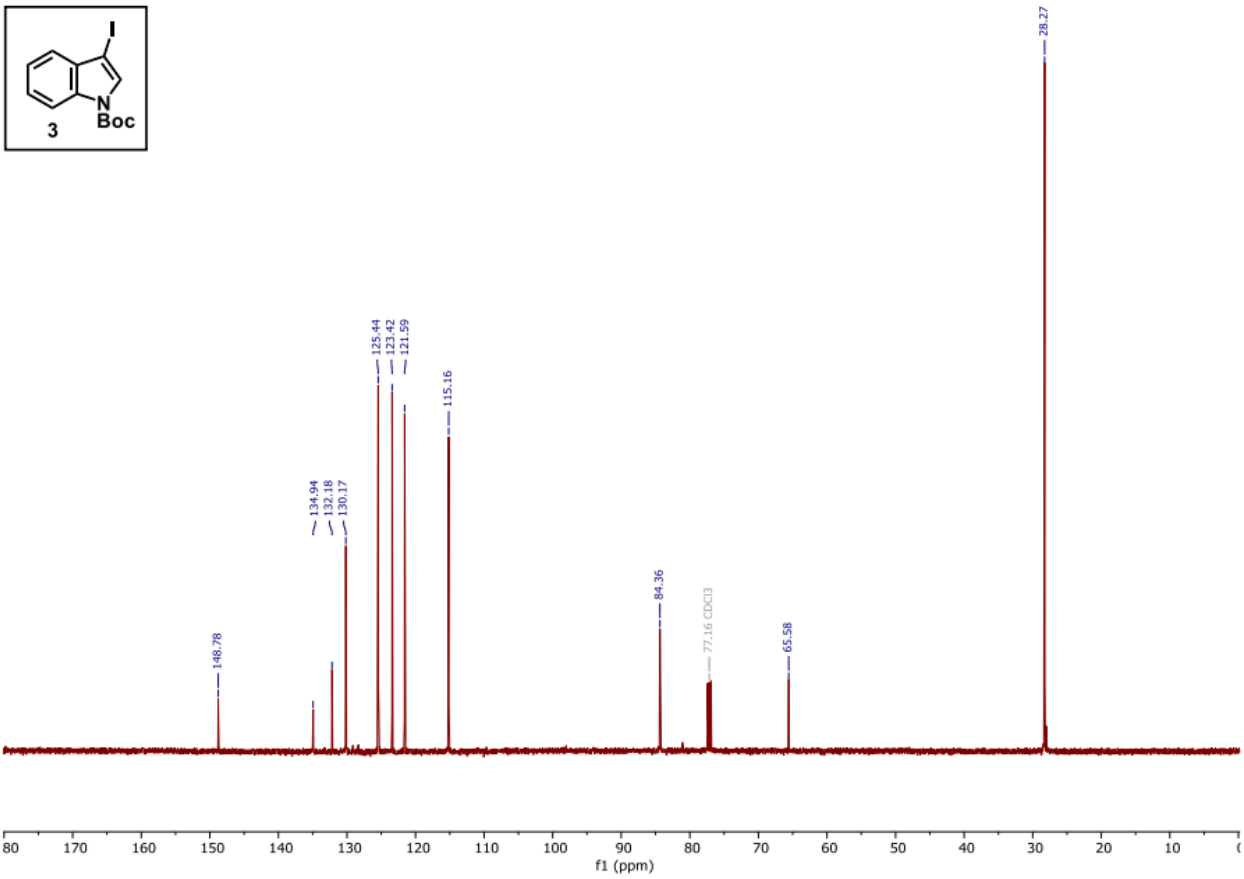
I
N
Boc
3
28.27
125.44
123.42
121.59
115.16
134.94
132.18
130.17
84.36
77.16 CDCl3
65.58
148.78
80
170
160
150
140
130
120
110
100
90
80
70
60
50
40
30
20
10
f1 (ppm)

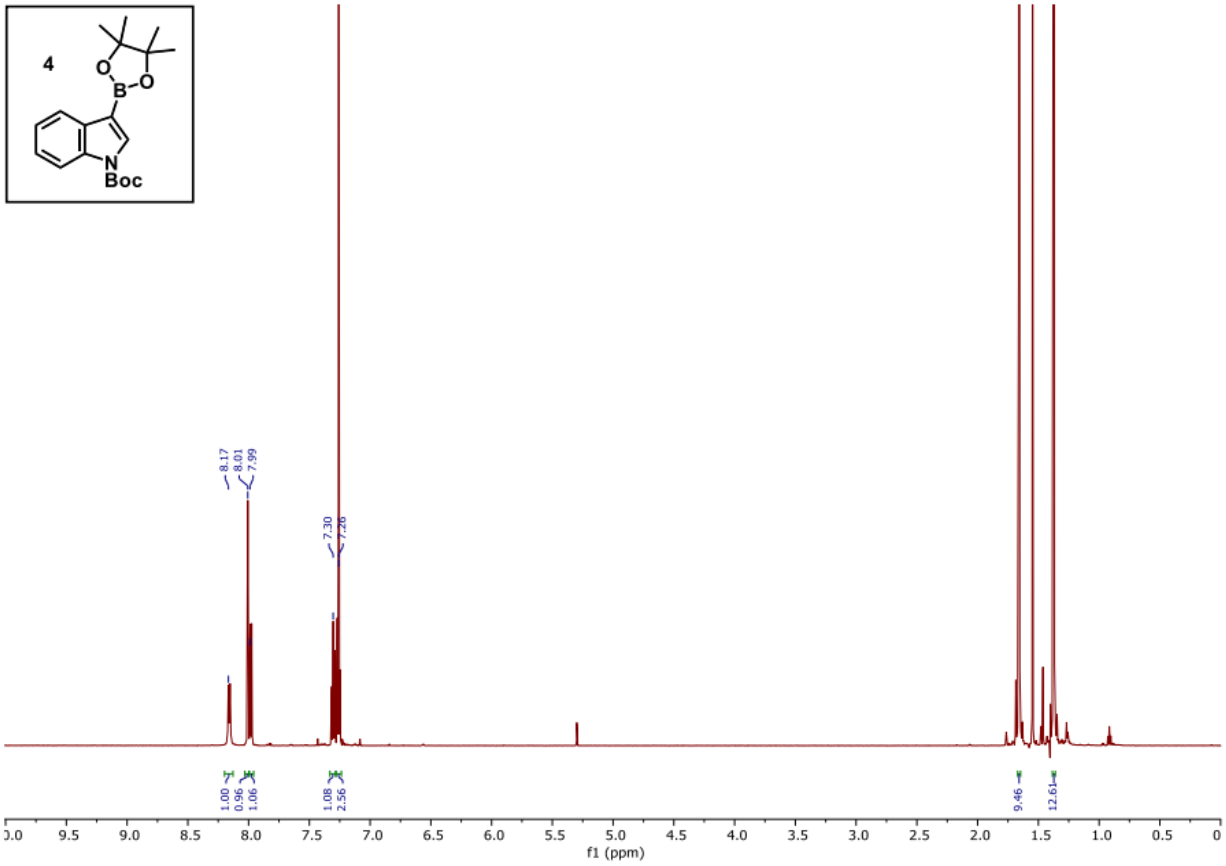
4
O
B
O
N
Boc
8.17
8.01
7.99
7.30
7.26
1.00
0.96
1.06
1.08
2.56
9.46
12.61
9.0
9.5
9.0
8.5
8.0
7.5
7.0
6.5
6.0
5.5
5.0
4.5
4.0
3.5
3.0
2.5
2.0
1.5
1.0
0.5
0
f1 (ppm)

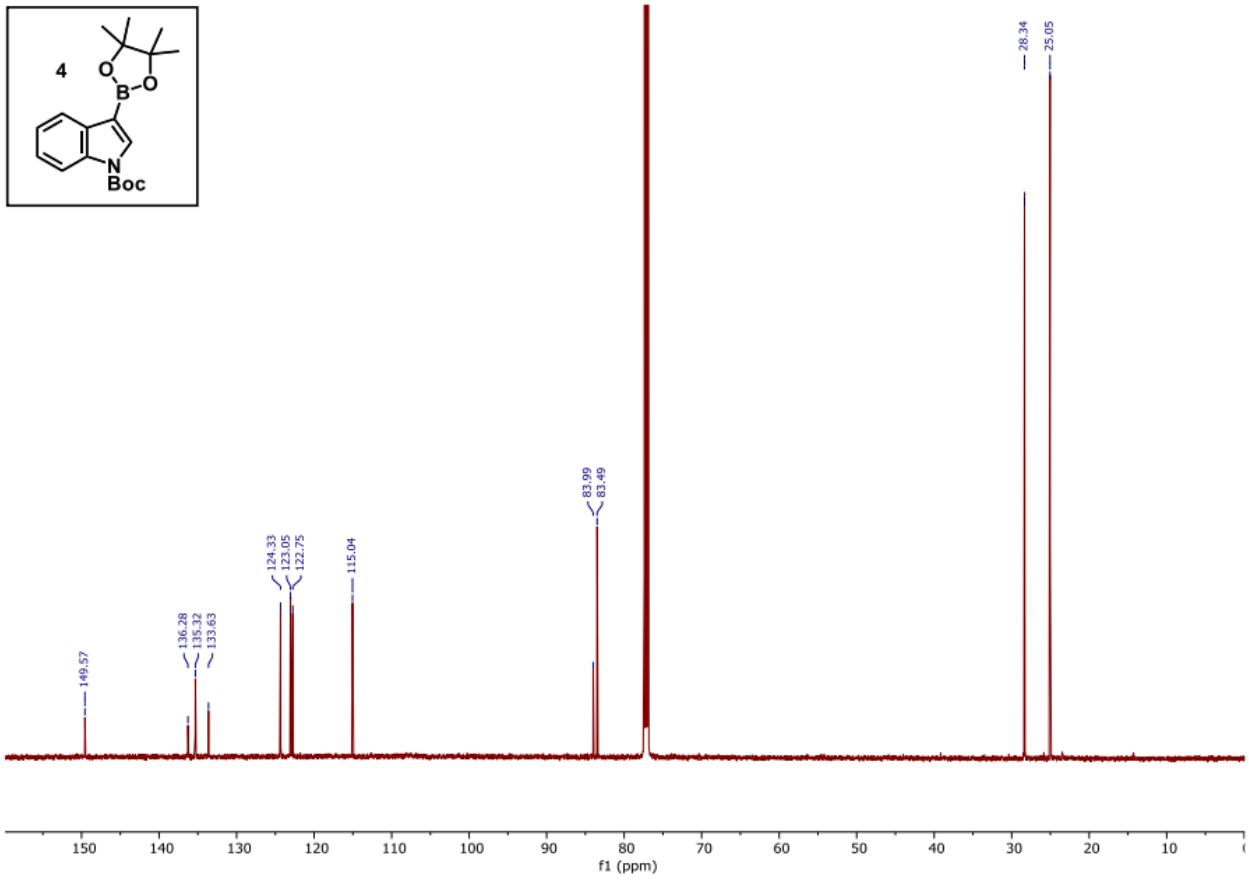
4
O
B
O
N
Boc
28.34
25.05
83.99
83.49
124.33
123.05
122.75
115.04
136.28
135.32
133.63
149.57
150
140
130
120
110
100
90
80
70
60
50
40
30
20
10
f1 (ppm)

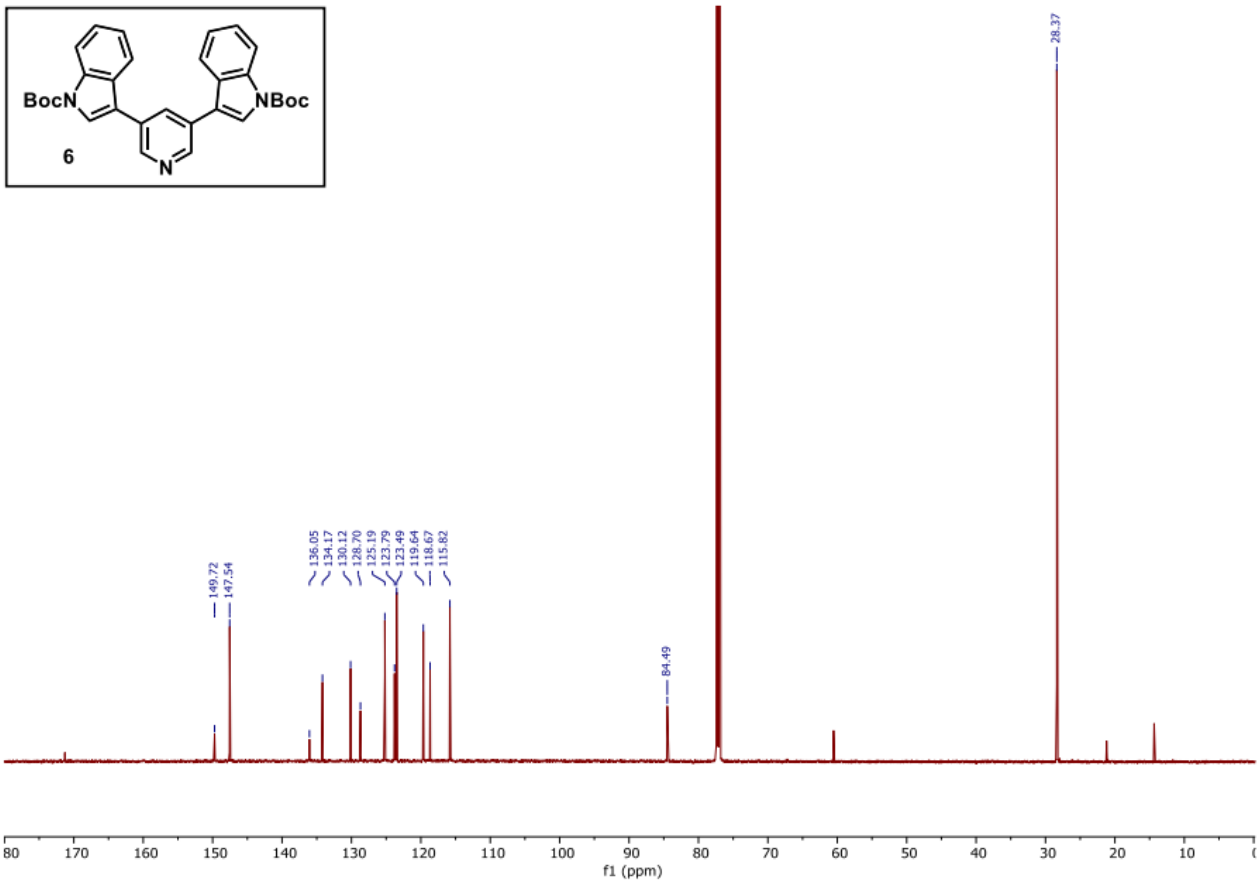
BocN
NBoc
N
6
149.72
147.54
136.05
134.17
130.12
128.70
125.19
123.79
123.49
119.64
118.67
115.82
84.49
28.37
80
170
160
150
140
130
120
110
100
90
80
70
60
50
40
30
20
10
f1 (ppm)

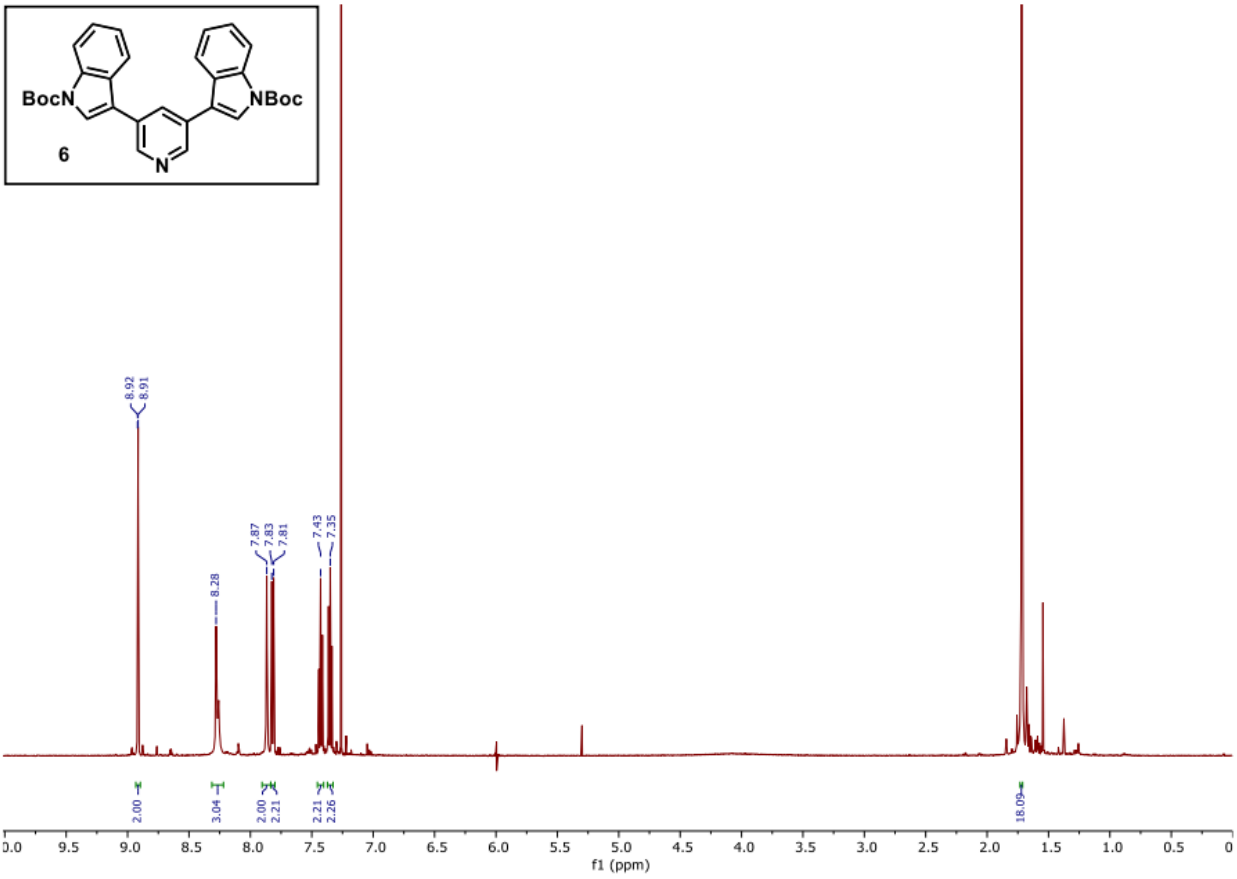
BocN
NBoc
N
6
8.92
8.91
8.28
7.87
7.83
7.81
7.43
7.35
2.00
3.04
2.00
2.21
2.21
2.26
18.09
f1 (ppm)

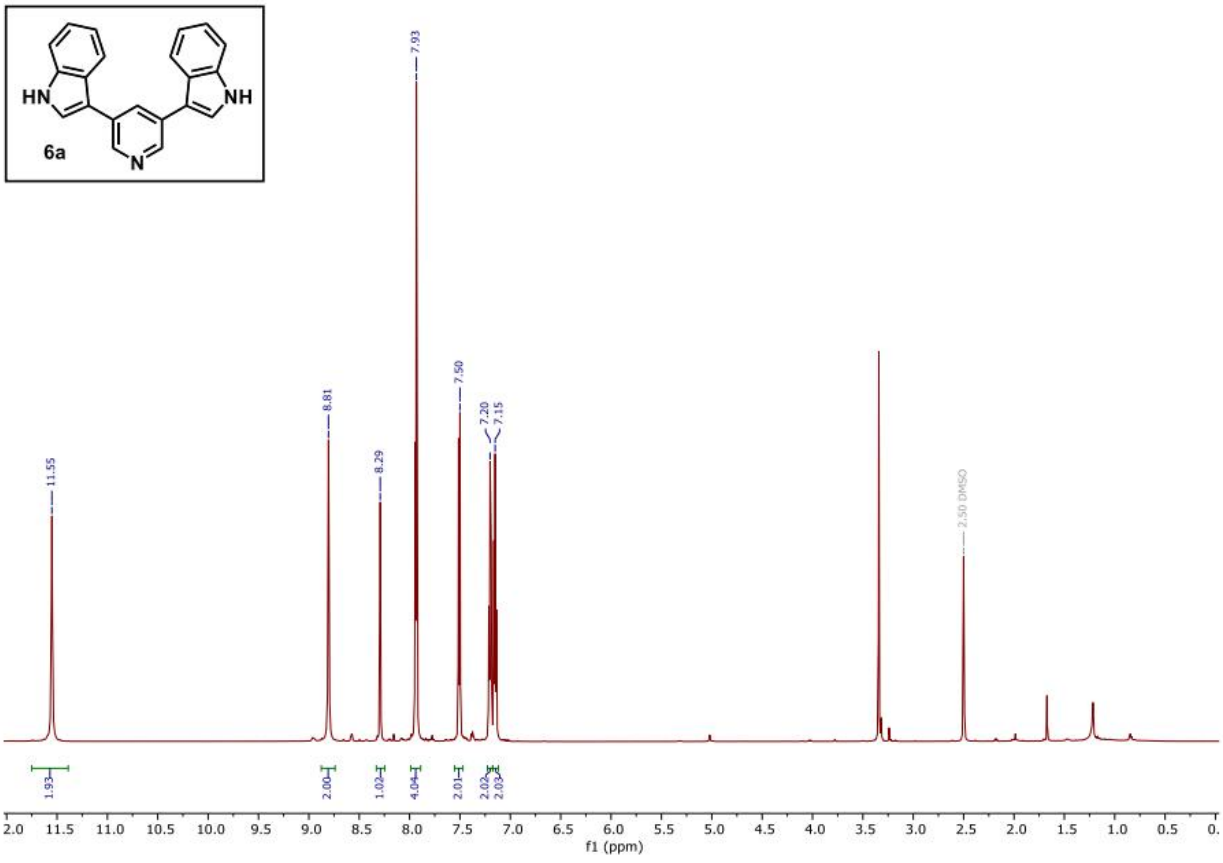
HN
NH
N
6a
11.55
8.81
8.29
7.93
7.50
7.20
7.15
2.50 DMSO
1.93
2.00
1.02
4.04
2.01
2.02
2.03
f1 (ppm)

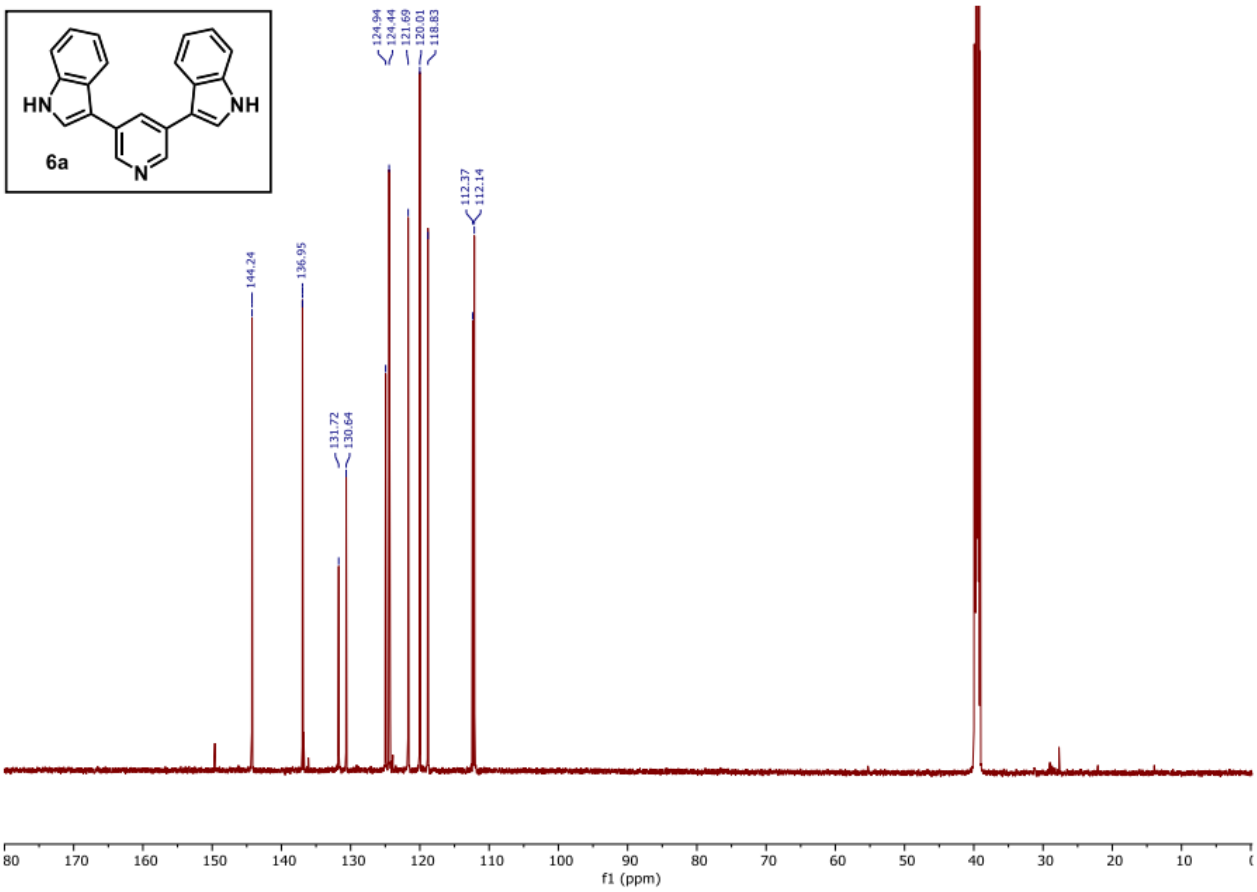
HN
NH
N
6a
144.24
136.95
131.72
130.64
124.94
124.44
121.69
120.01
118.83
112.37
112.14
80
170
160
150
140
130
120
110
100
90
80
70
60
50
40
30
20
10
f1 (ppm)

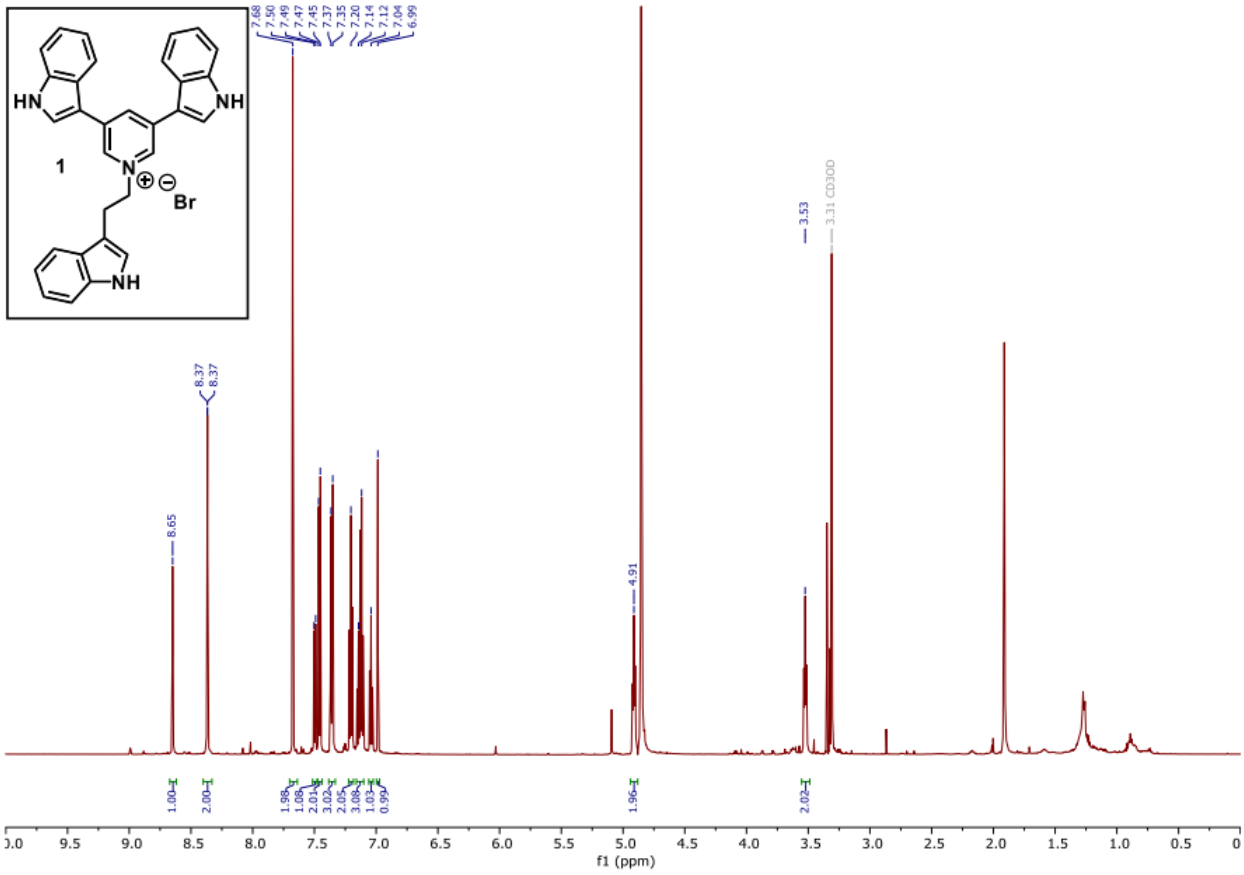
HN
NH
1
N
Br
NH
8.65
8.37
8.37
4.91
3.53
3.31 CD3OD
f1 (ppm)

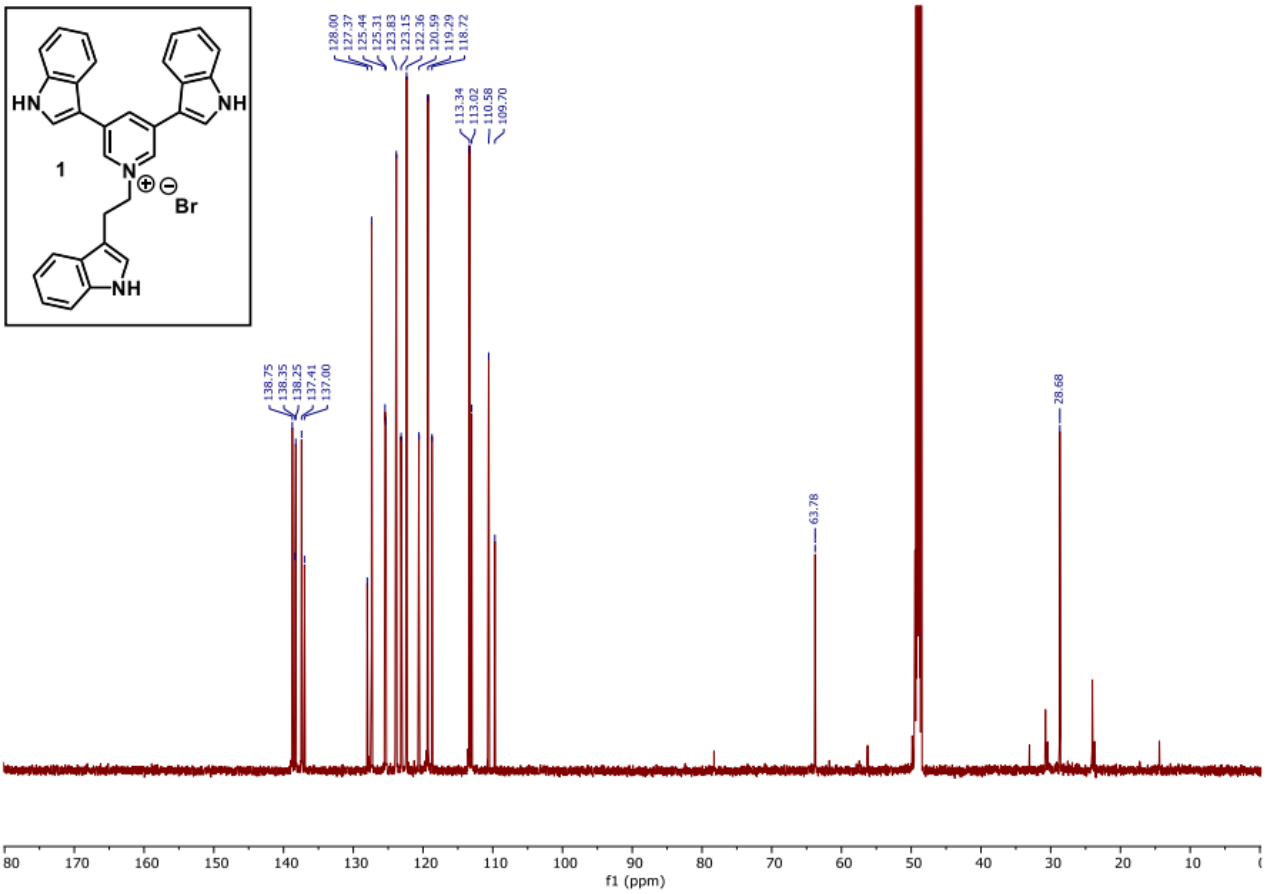
HN
NH
1
N
Br
NH
128.00
127.37
125.44
125.31
123.83
123.15
122.36
120.59
119.29
118.72
113.34
113.02
110.58
109.70
138.75
138.35
138.25
137.41
137.00
63.78
28.68
f1 (ppm)

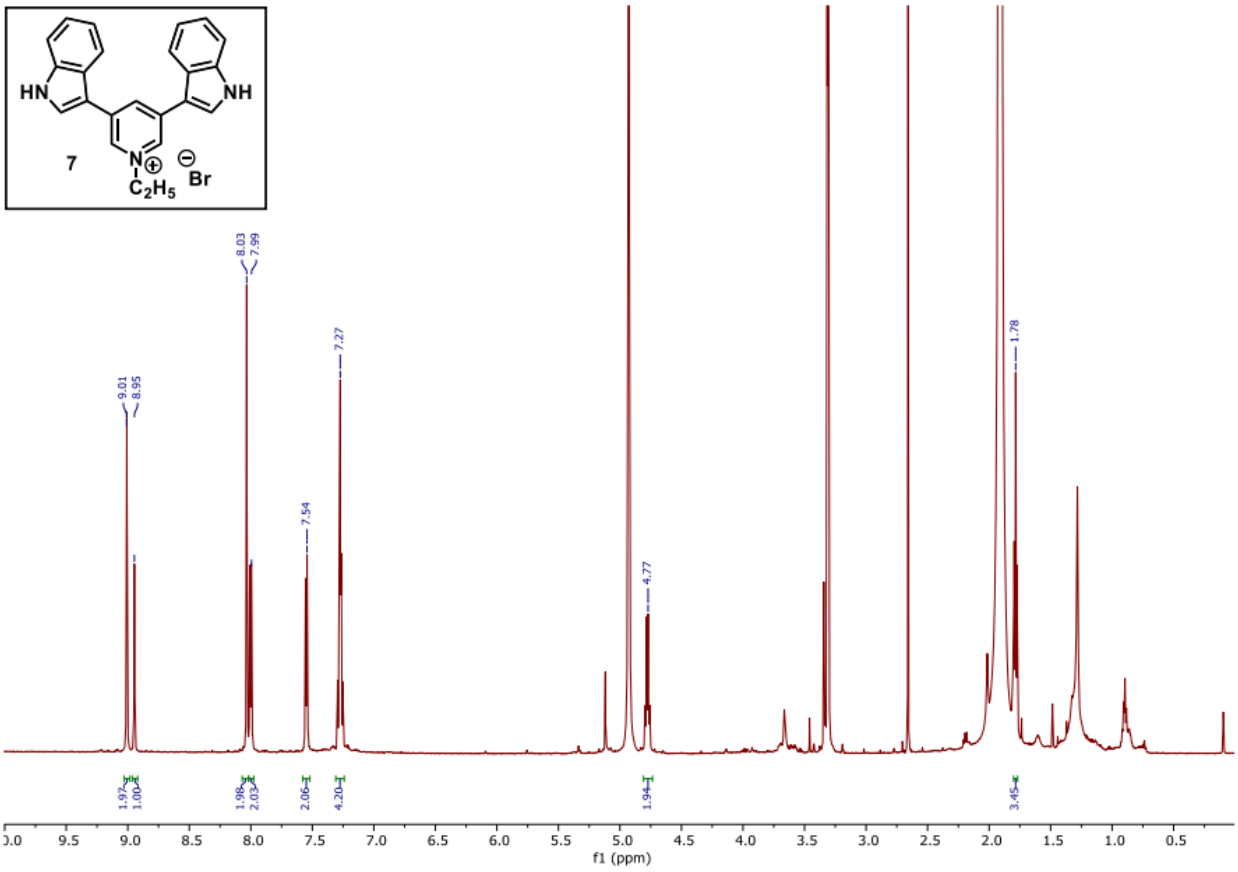
HN
NH
7
N
Br
C2H5
9.01
8.95
8.03
7.99
7.54
7.27
4.77
1.78
1.97
1.00
1.98
2.03
2.06
4.20
1.94
3.45
f1 (ppm)

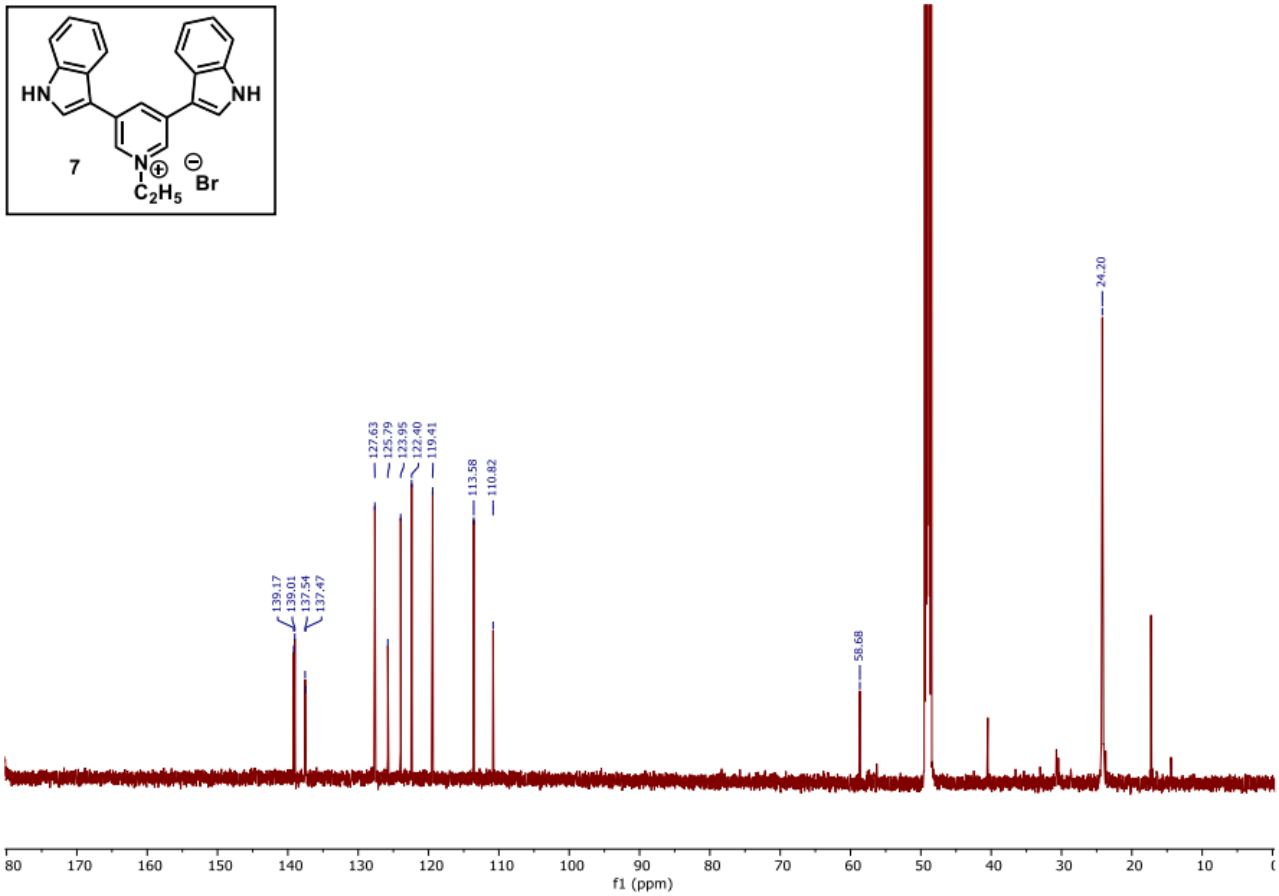
HN
NH
7
N
C2H5
Br
139.17
139.01
137.54
137.47
127.63
125.79
123.95
122.40
119.41
113.58
110.82
58.68
24.20
80
170
160
150
140
130
120
110
100
90
80
70
60
50
40
30
20
10
f1 (ppm)

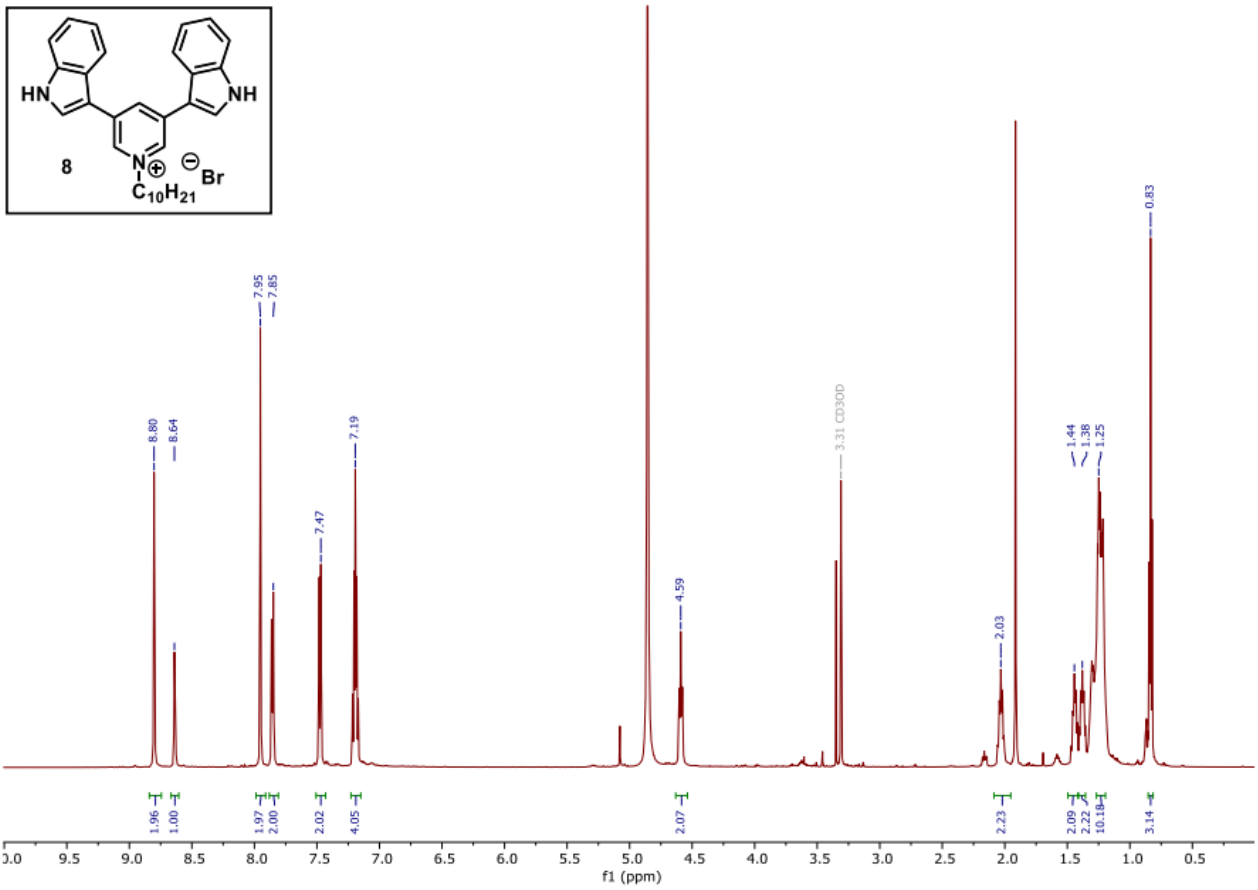
HN
NH
8
N
Br
C10H21
8.80
8.64
7.95
7.85
7.47
7.19
4.59
3.31 CD3OD
2.03
1.44
1.38
1.25
0.83
1.96
1.00
1.97
2.00
2.02
4.05
2.07
2.23
2.09
2.22
10.18
3.14
f1 (ppm)

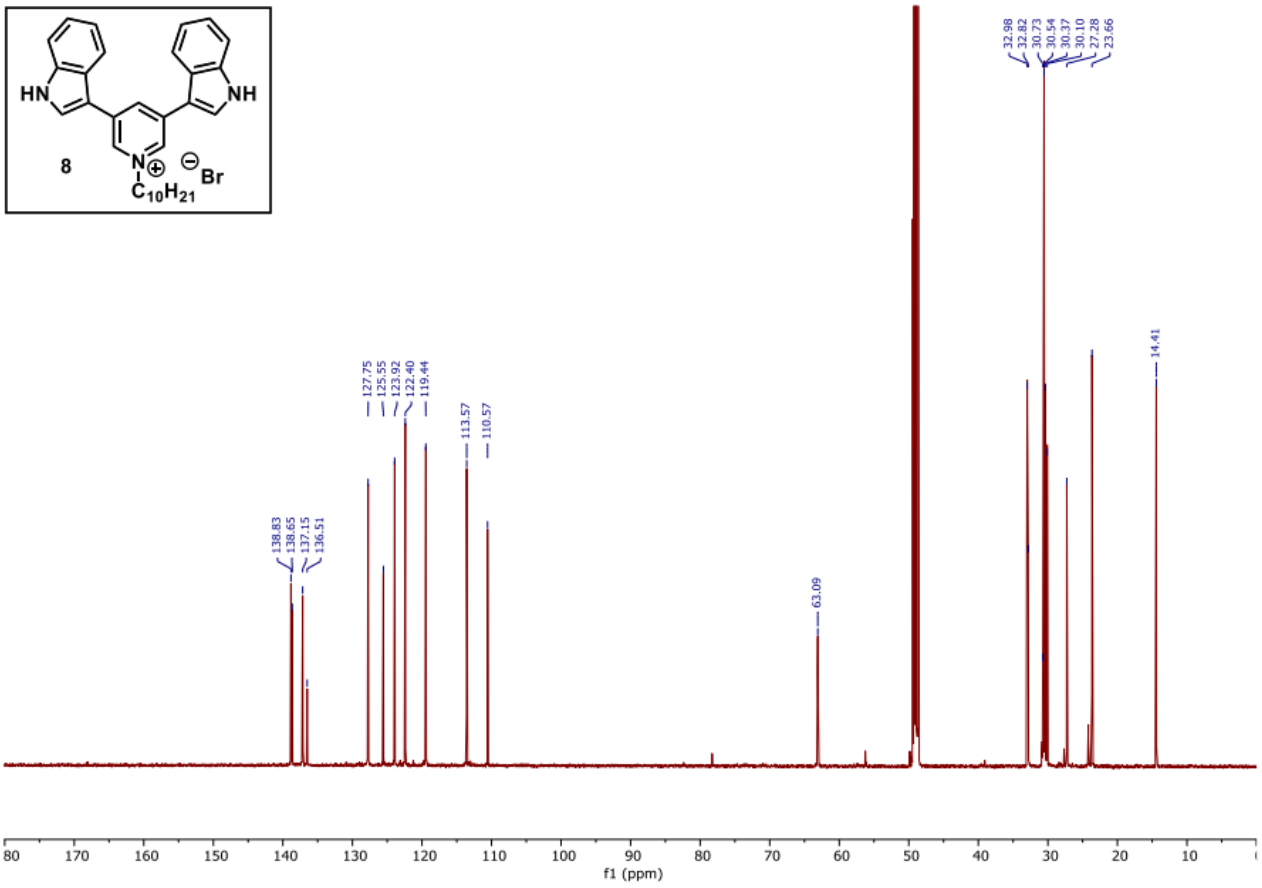
HN
NH
8
N
Br
C10H21
32.98
32.82
30.73
30.54
30.37
30.10
27.28
23.66
14.41
127.75
125.55
123.92
122.40
119.44
113.57
110.57
138.83
138.65
137.15
136.51
63.09
80
170
160
150
140
130
120
110
100
90
80
70
60
50
40
30
20
10
f1 (ppm)

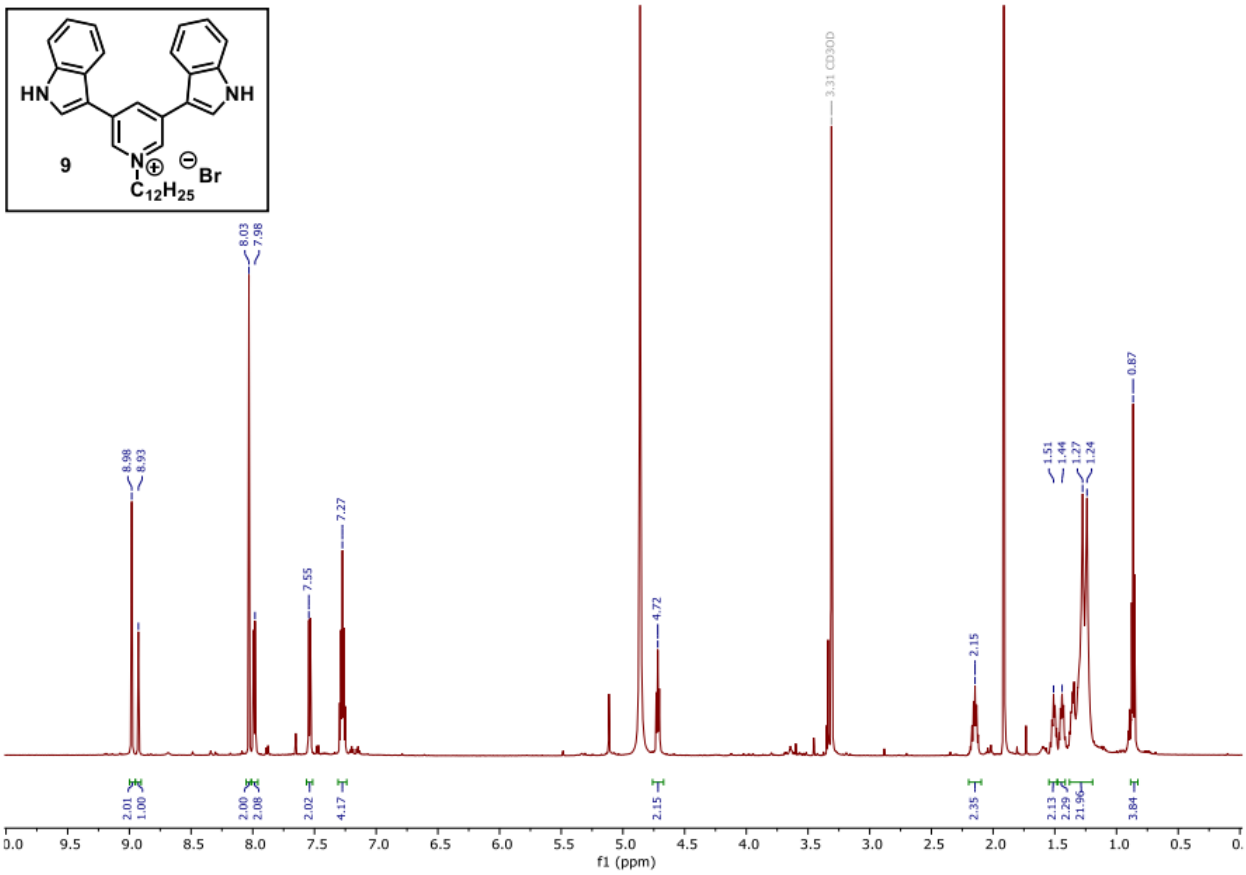
HN
NH
9
N
Br
C12H25
8.98
8.93
8.03
7.98
7.55
7.27
4.72
3.31 CD3OD
2.15
1.51
1.44
1.27
1.24
0.87
2.01
1.00
2.00
2.08
2.02
4.17
2.15
2.35
2.13
2.29
21.96
3.84
f1 (ppm)

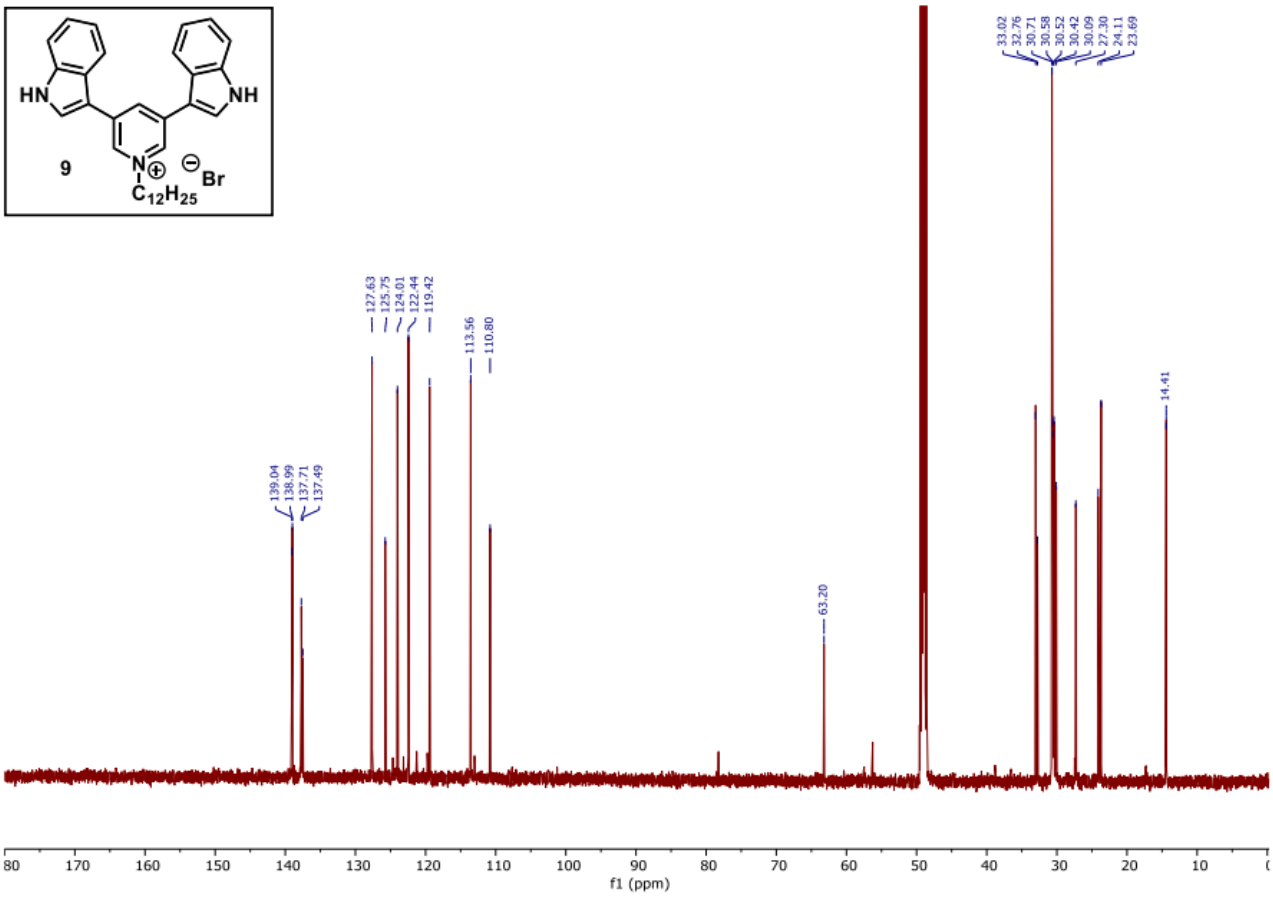
HN
NH
9
N
Br
C12H25
33.02
32.76
30.71
30.58
30.52
30.42
30.09
27.30
24.11
23.69
14.41
63.20
139.04
138.99
137.71
137.49
127.63
125.75
124.01
122.44
119.42
113.56
110.80
80
170
160
150
140
130
120
110
100
90
80
70
60
50
40
30
20
10
f1 (ppm)

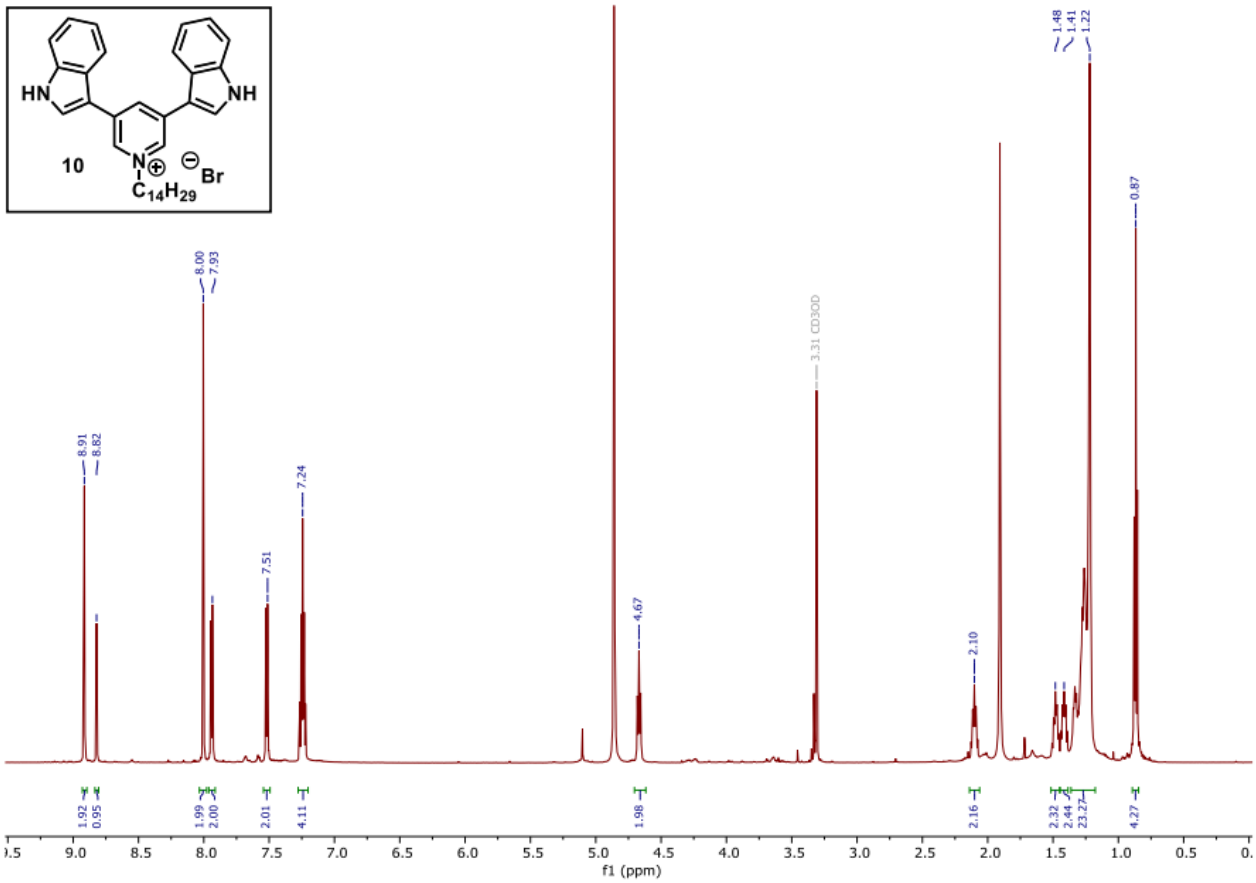
HN
NH
10
N
Br
C14H29
8.91
8.82
8.00
7.93
7.51
7.24
3.31 CD3OD
4.67
2.10
1.48
1.41
1.22
0.87
1.92
0.95
1.99
2.00
2.01
4.11
1.98
2.16
2.32
2.44
23.27
4.27
f1 (ppm)

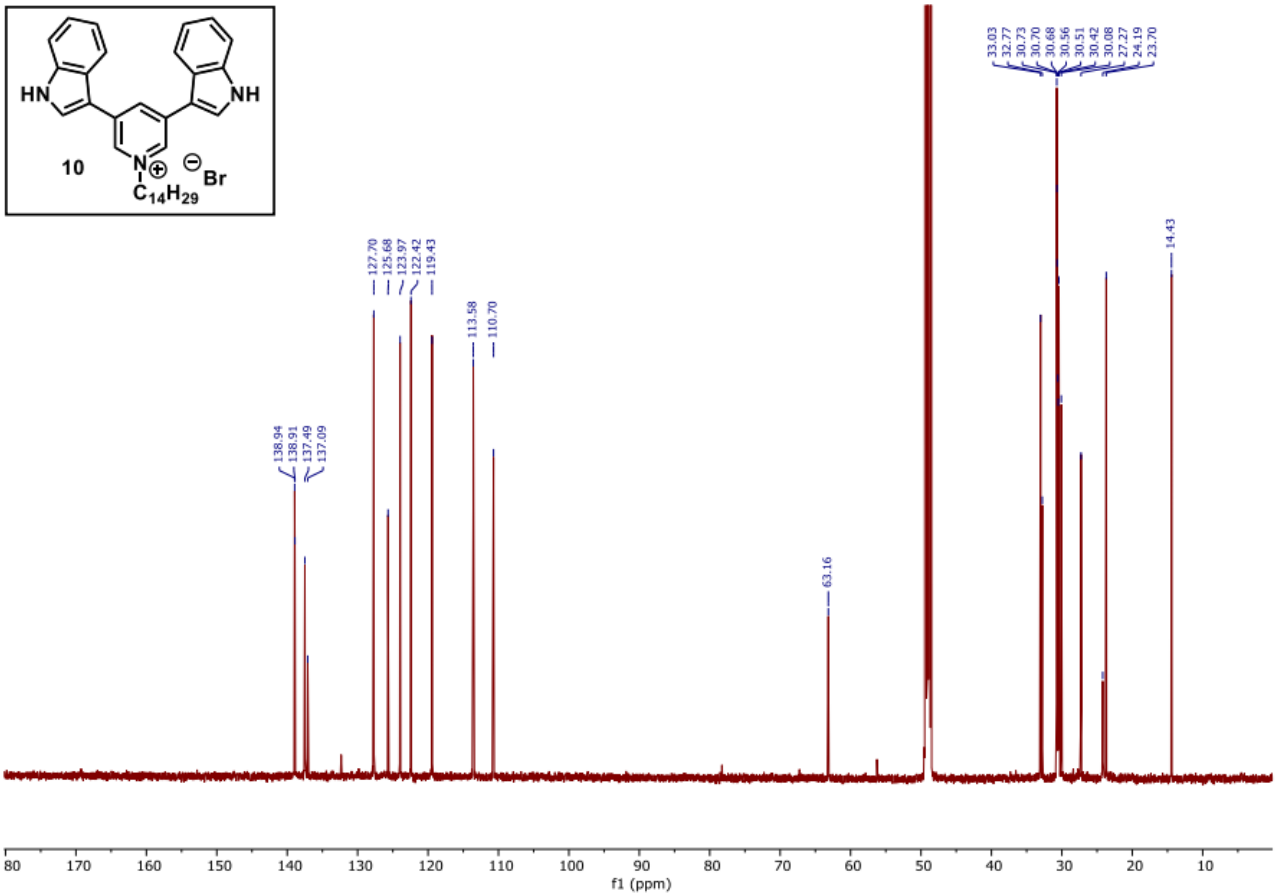
HN
NH
10
N
Br
C14H29
33.03
32.77
30.73
30.70
30.68
30.56
30.51
30.42
30.08
27.27
24.19
23.70
14.43
127.70
125.68
123.97
122.42
119.43
113.58
110.70
138.94
138.91
137.49
137.09
63.16
80
170
160
150
140
130
120
110
100
90
80
70
60
50
40
30
20
10
f1 (ppm)

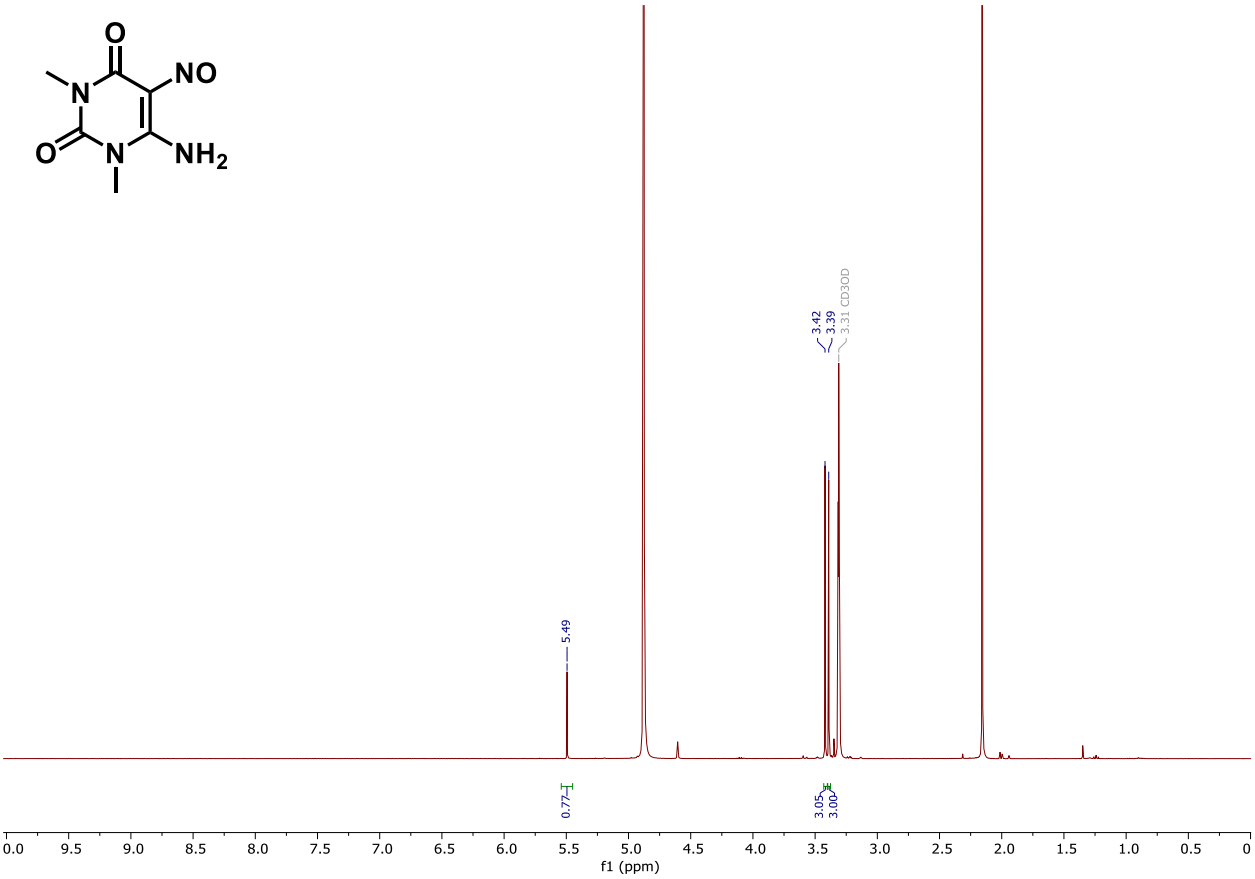
O
NO
N
O
N
NH2
3.42
3.39
3.31 CD3OD
5.49
0.77
3.05
3.00
0.0
9.5
9.0
8.5
8.0
7.5
7.0
6.5
6.0
5.5
5.0
4.5
4.0
3.5
3.0
2.5
2.0
1.5
1.0
0.5
0
f1 (ppm)

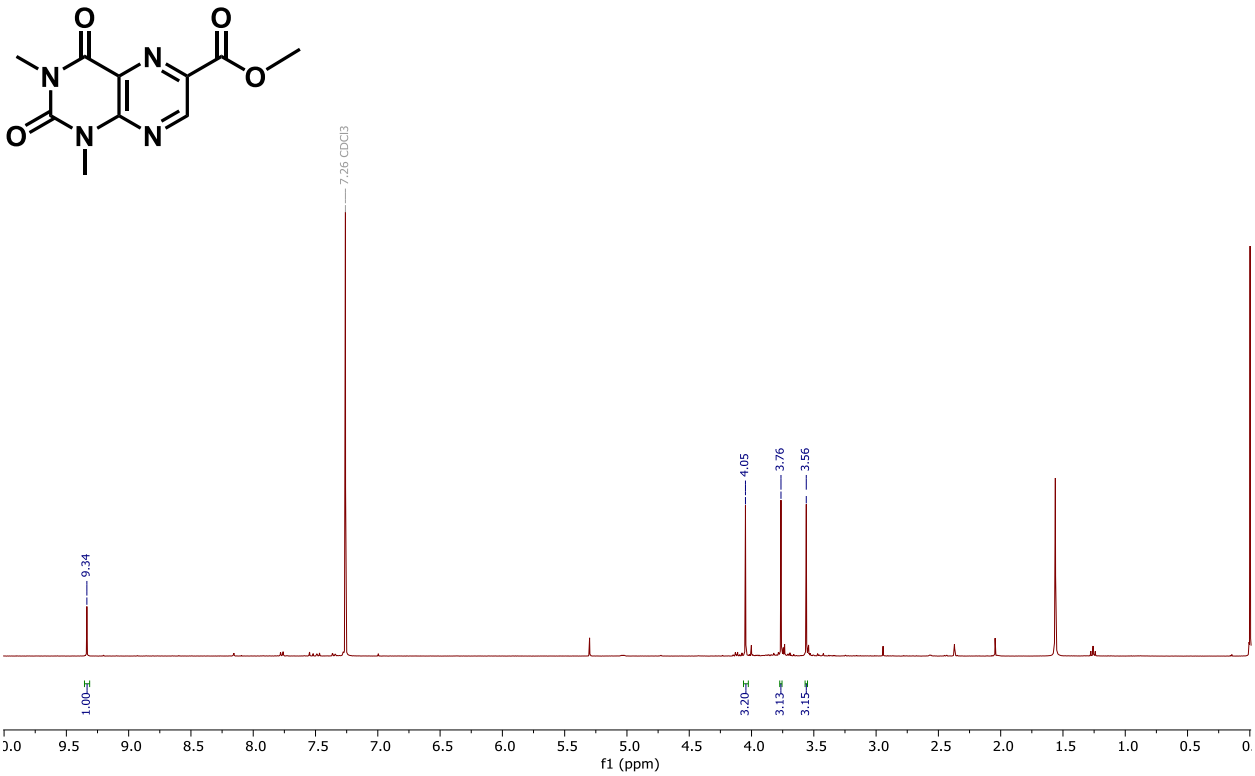
O
O
N
N
O
O
N
N
7.26 CDCl3
9.34
4.05
3.76
3.56
1.00
3.20
3.13
3.15
f1 (ppm)

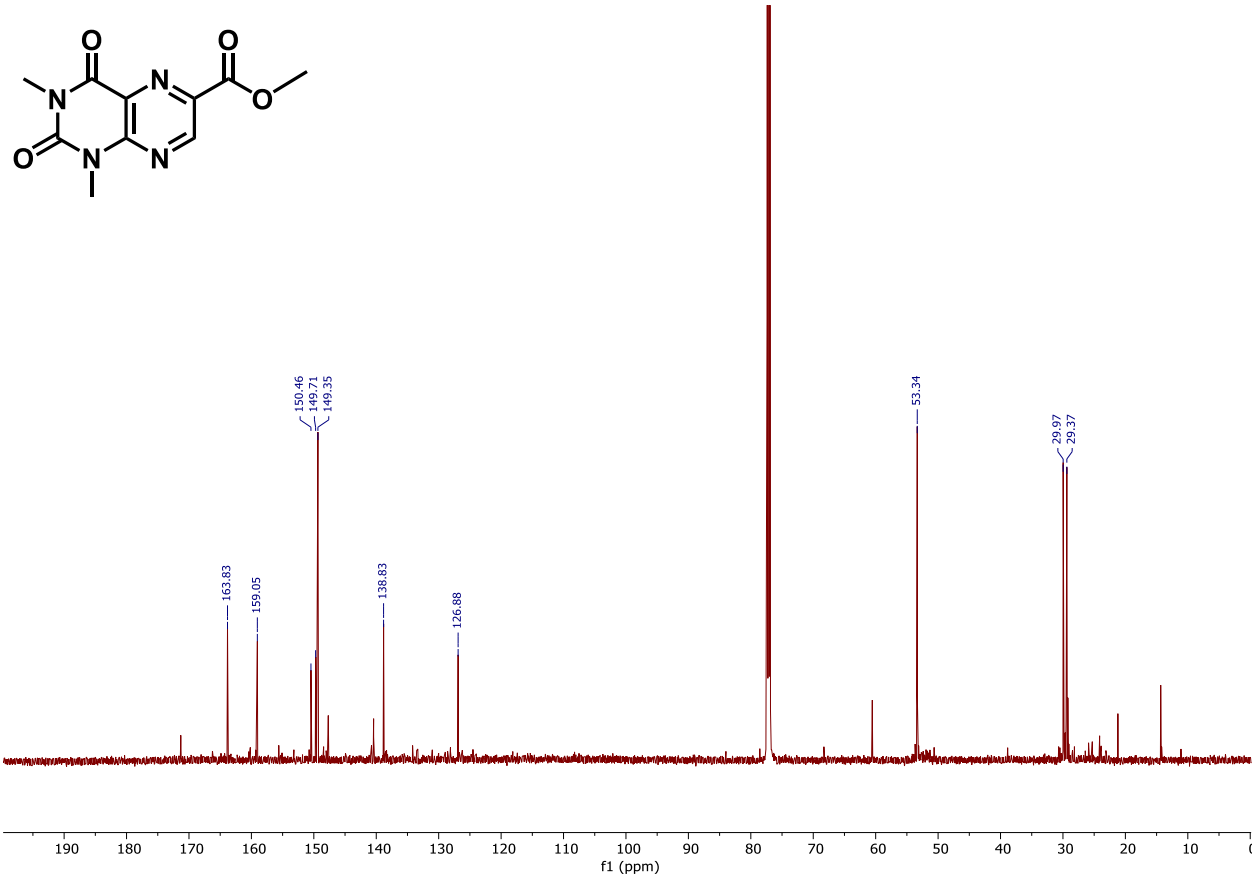
O
O
N
N
O
O
N
N
150.46
149.71
149.35
163.83
159.05
138.83
126.88
53.34
29.97
29.37
190
180
170
160
150
140
130
120
110
100
90
80
70
60
50
40
30
20
10
f1 (ppm)

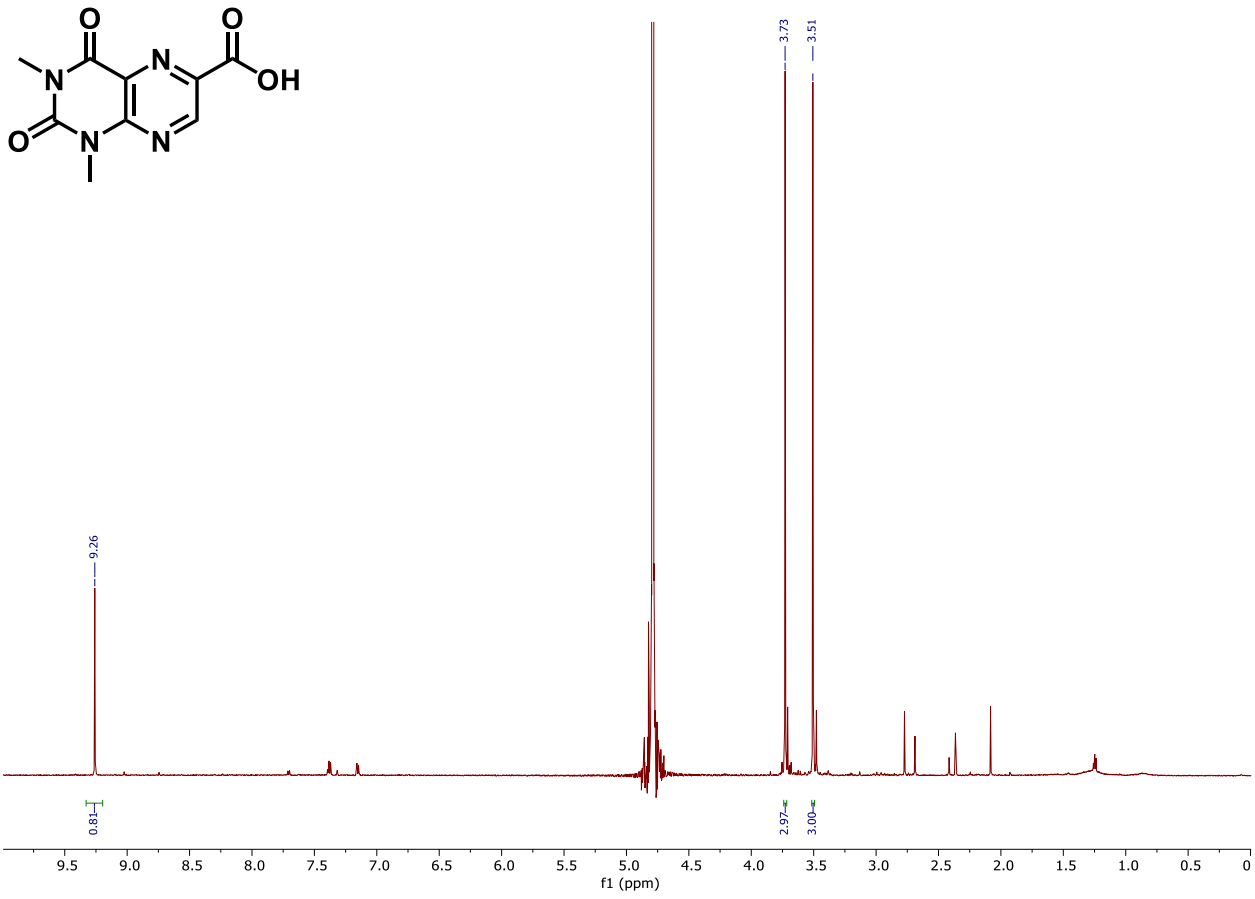
O
O
N
OH
N
O
N
N
3.73
3.51
9.26
0.81
2.97
3.00
9.5
9.0
8.5
8.0
7.5
7.0
6.5
6.0
5.5
5.0
4.5
4.0
3.5
3.0
2.5
2.0
1.5
1.0
0.5
0
f1 (ppm)

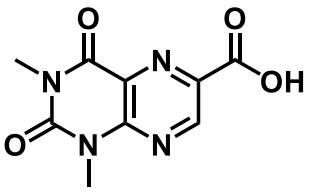
O
O
N
N
OH
O
N
N

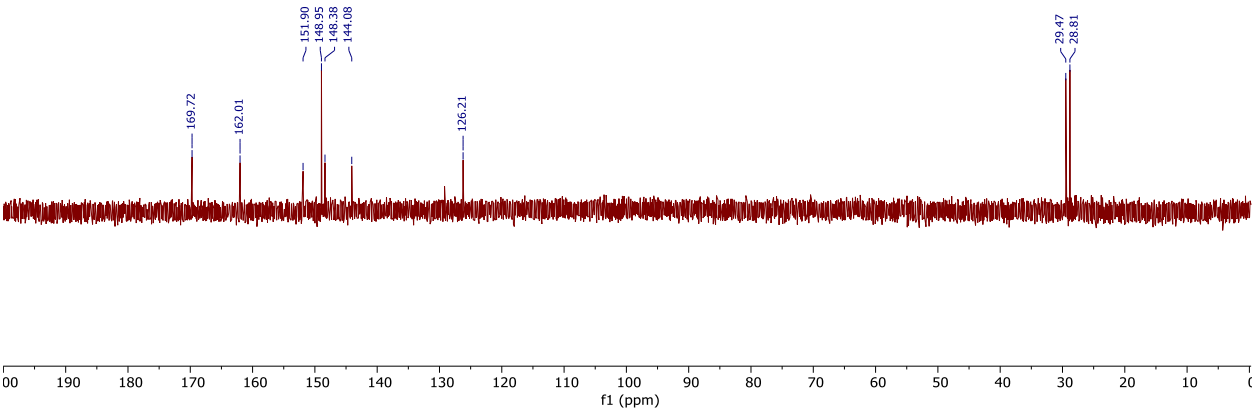
169.72
162.01
151.90
148.95
148.38
144.08
126.21
29.47
28.81
f1 (ppm)

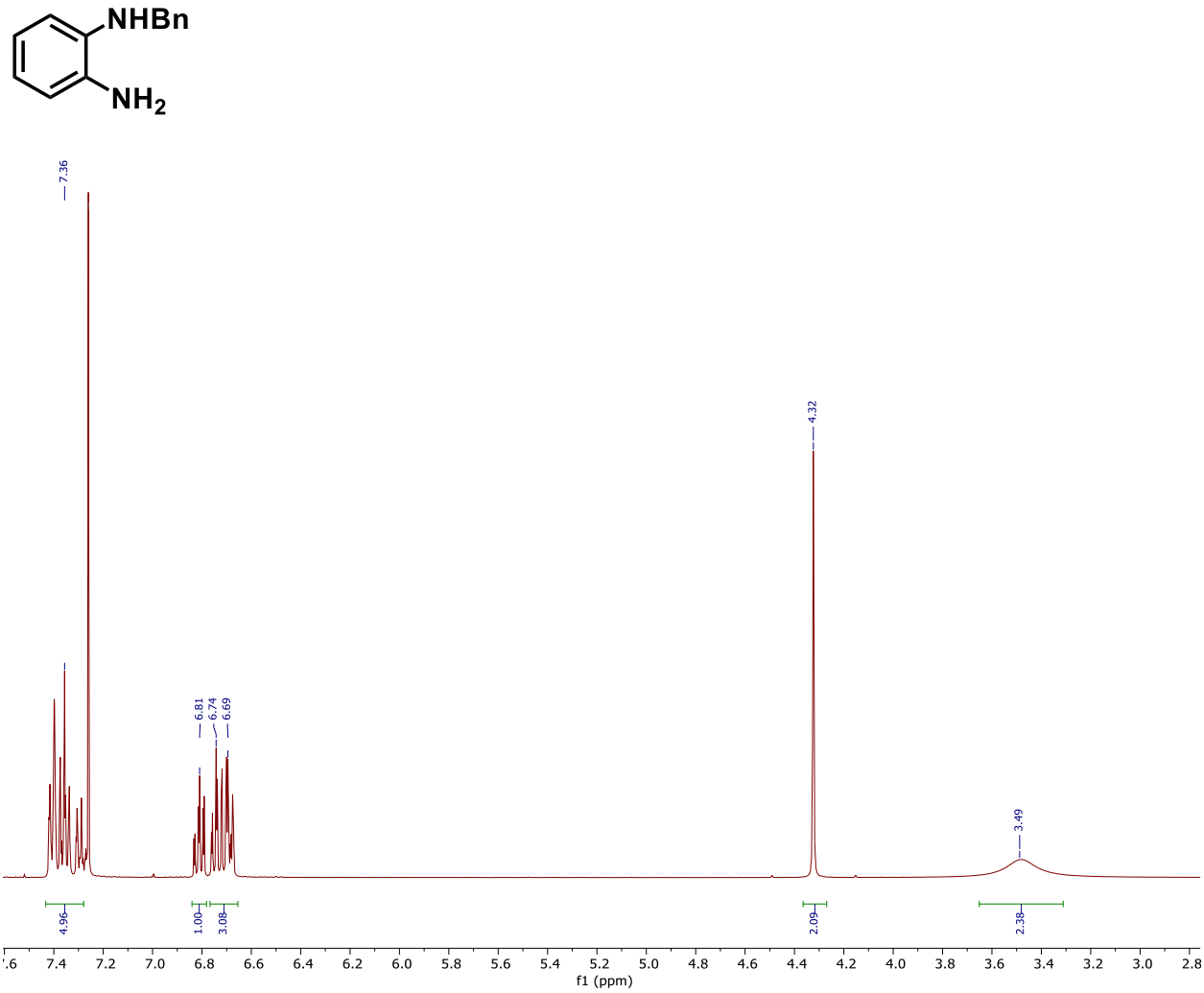
NHBn
NH2
7.36
6.81
6.74
6.69
4.32
3.49
4.96
1.00
3.08
2.09
2.38
f1 (ppm)

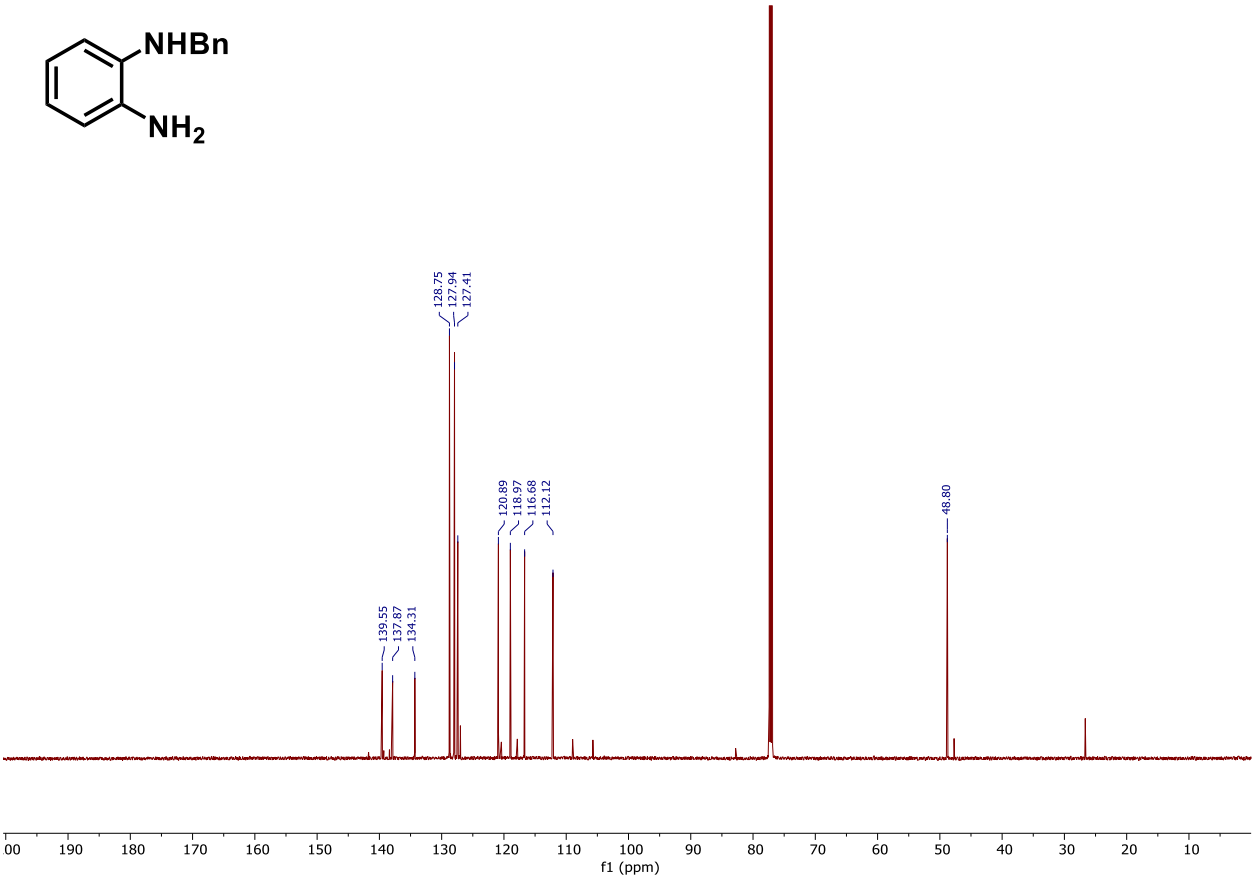
NHBn
NH2
128.75
127.94
127.41
120.89
118.97
116.68
112.12
48.80
139.55
137.87
134.31
f1 (ppm)

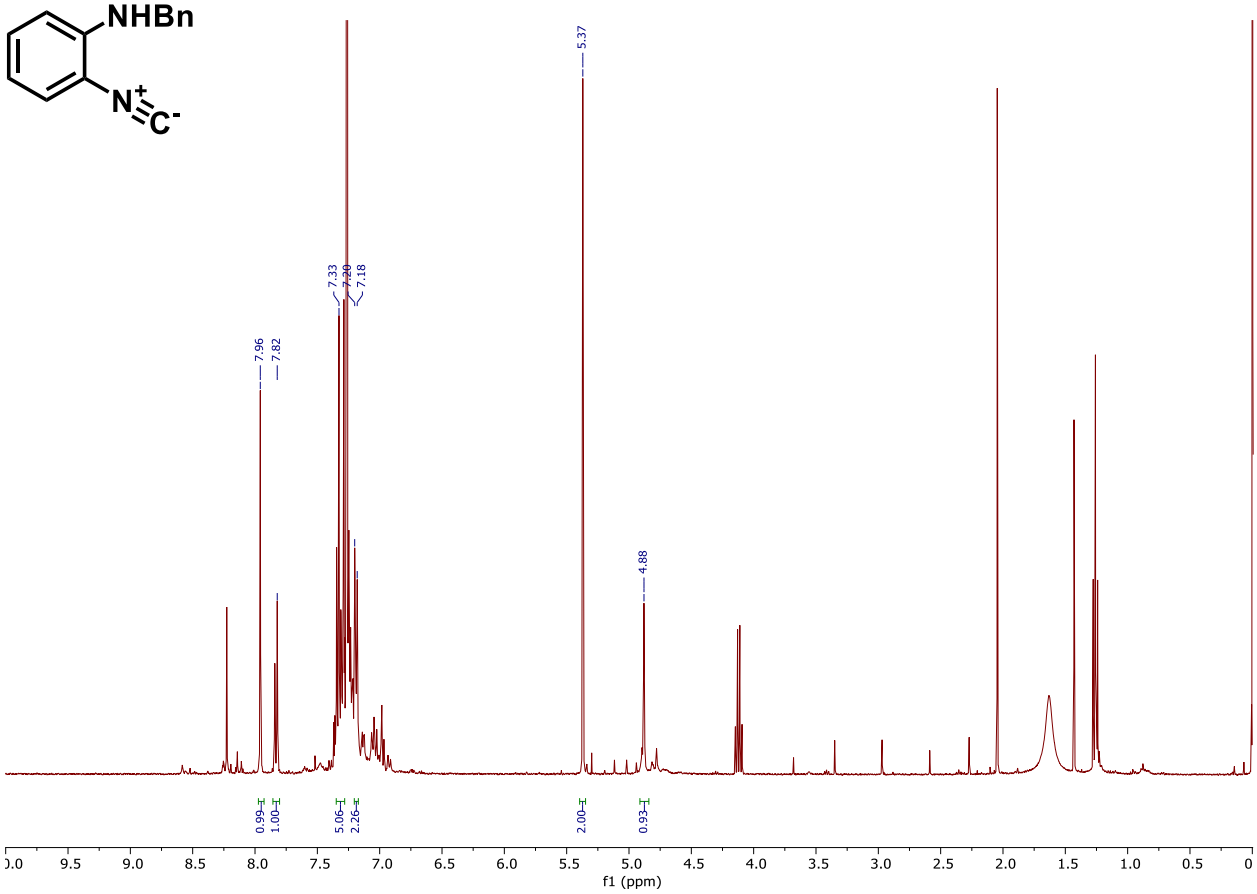
NHBn
N+
C-
7.96
7.82
7.33
7.20
7.18
5.37
4.88
0.99
1.00
5.06
2.26
2.00
0.93
f1 (ppm)

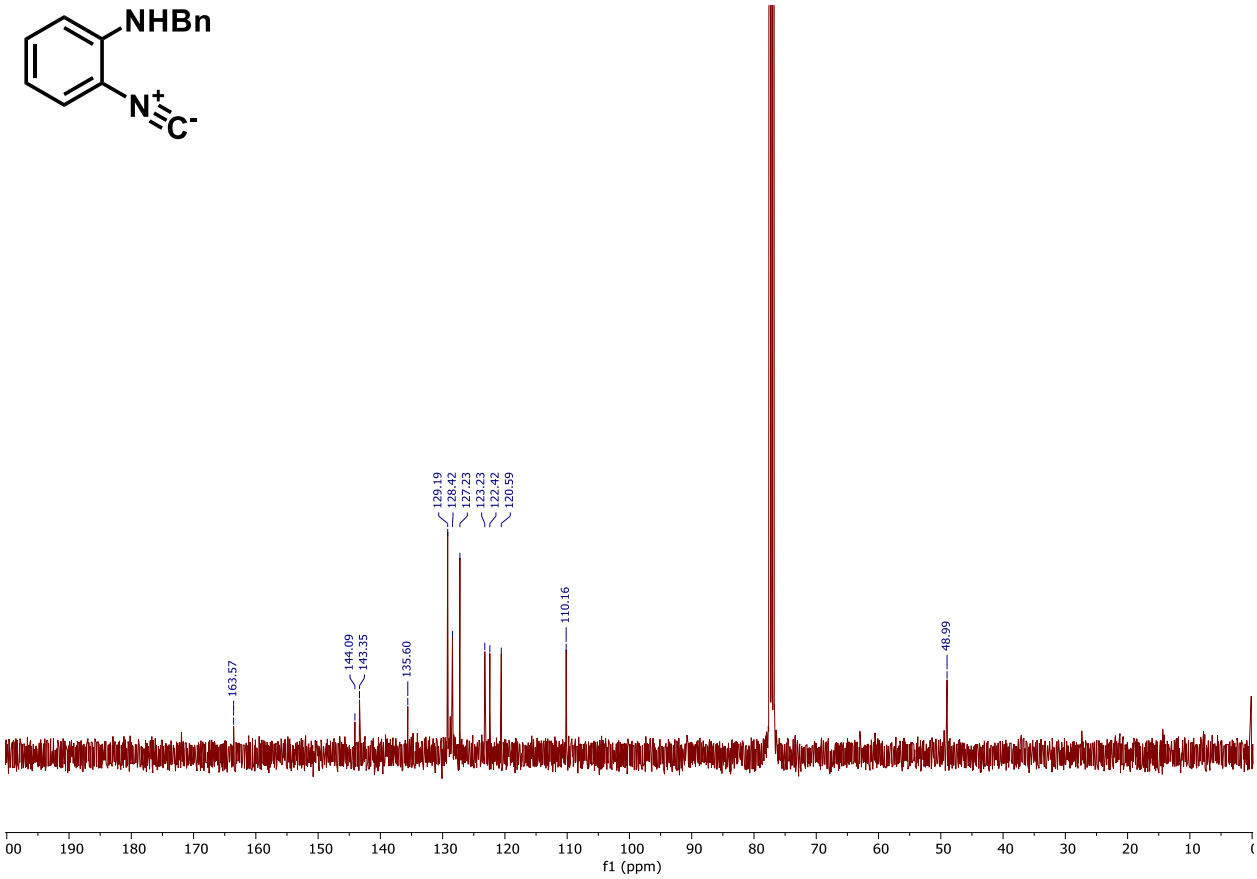
NHBn
N+
C-
163.57
144.09
143.35
135.60
129.19
128.42
127.23
123.23
122.42
120.59
110.16
48.99
f1 (ppm)

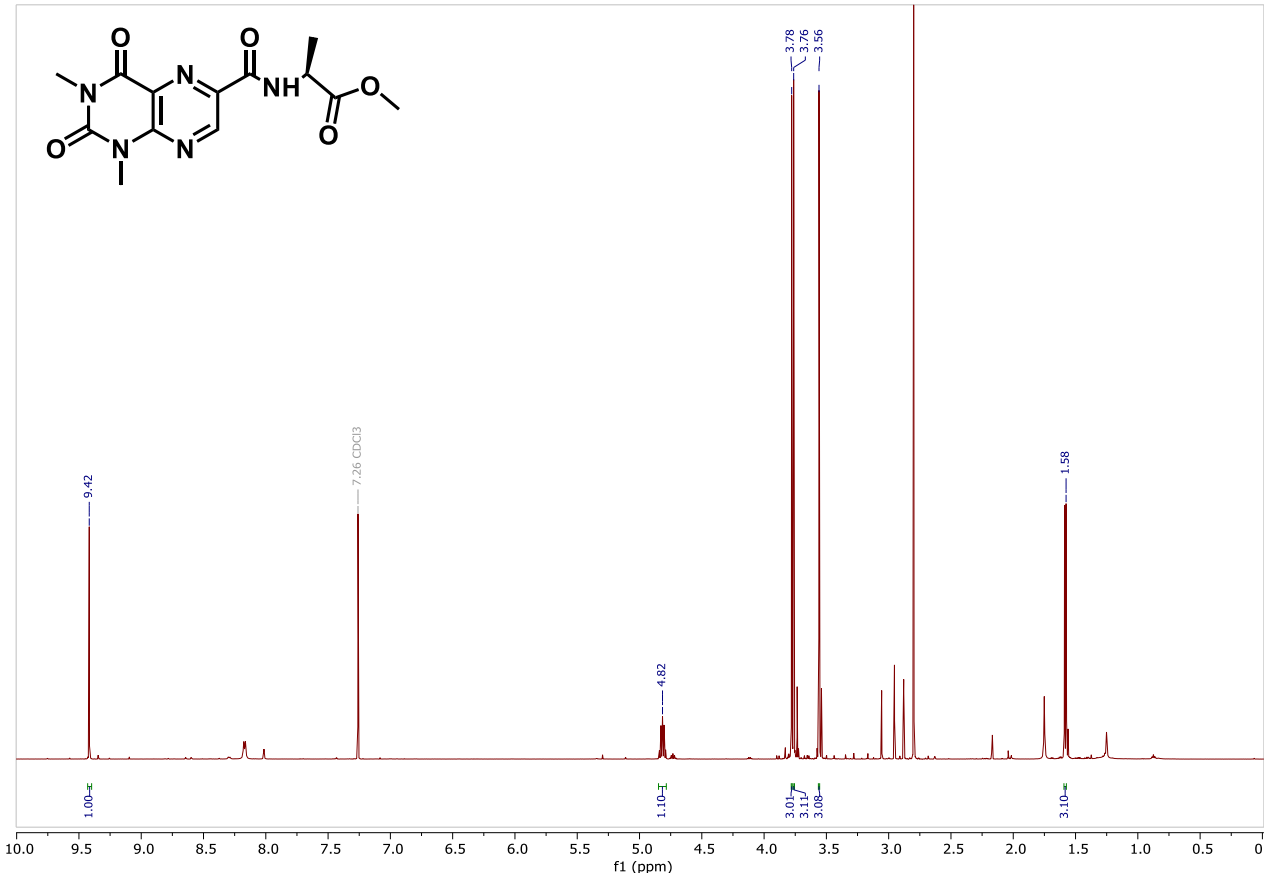
O
O
N
NH
O
N
O
N
N
O
9.42
7.26 CDCl3
4.82
3.78
3.76
3.56
1.58
1.00
1.10
3.01
3.11
3.08
3.10
10.0 9.5 9.0 8.5 8.0 7.5 7.0 6.5 6.0 5.5 5.0 4.5 4.0 3.5 3.0 2.5 2.0 1.5 1.0 0.5 0
f1 (ppm)

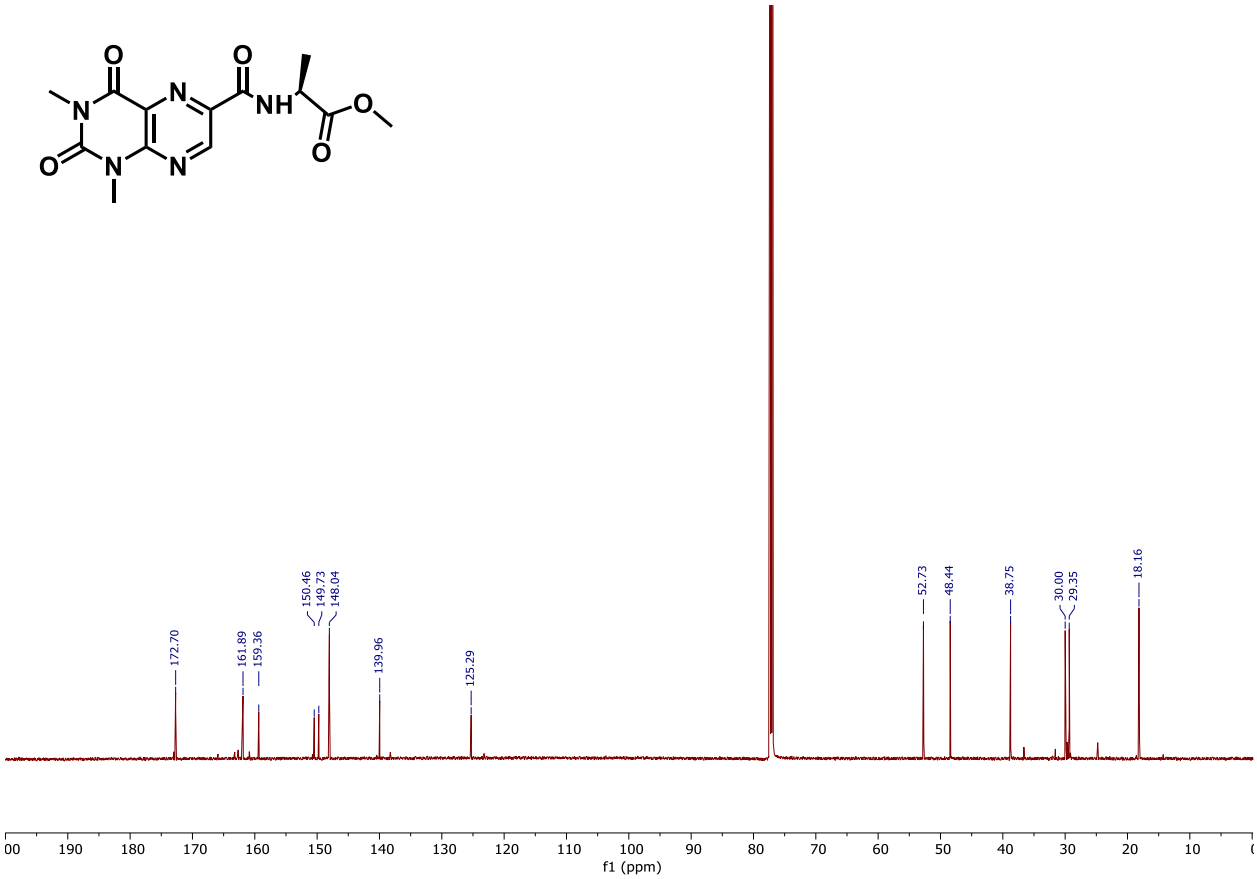
O
O
N
NH
O
O
O
N
N
N
172.70
161.89
159.36
150.46
149.73
148.04
139.96
125.29
52.73
48.44
38.75
30.00
29.35
18.16
f1 (ppm)

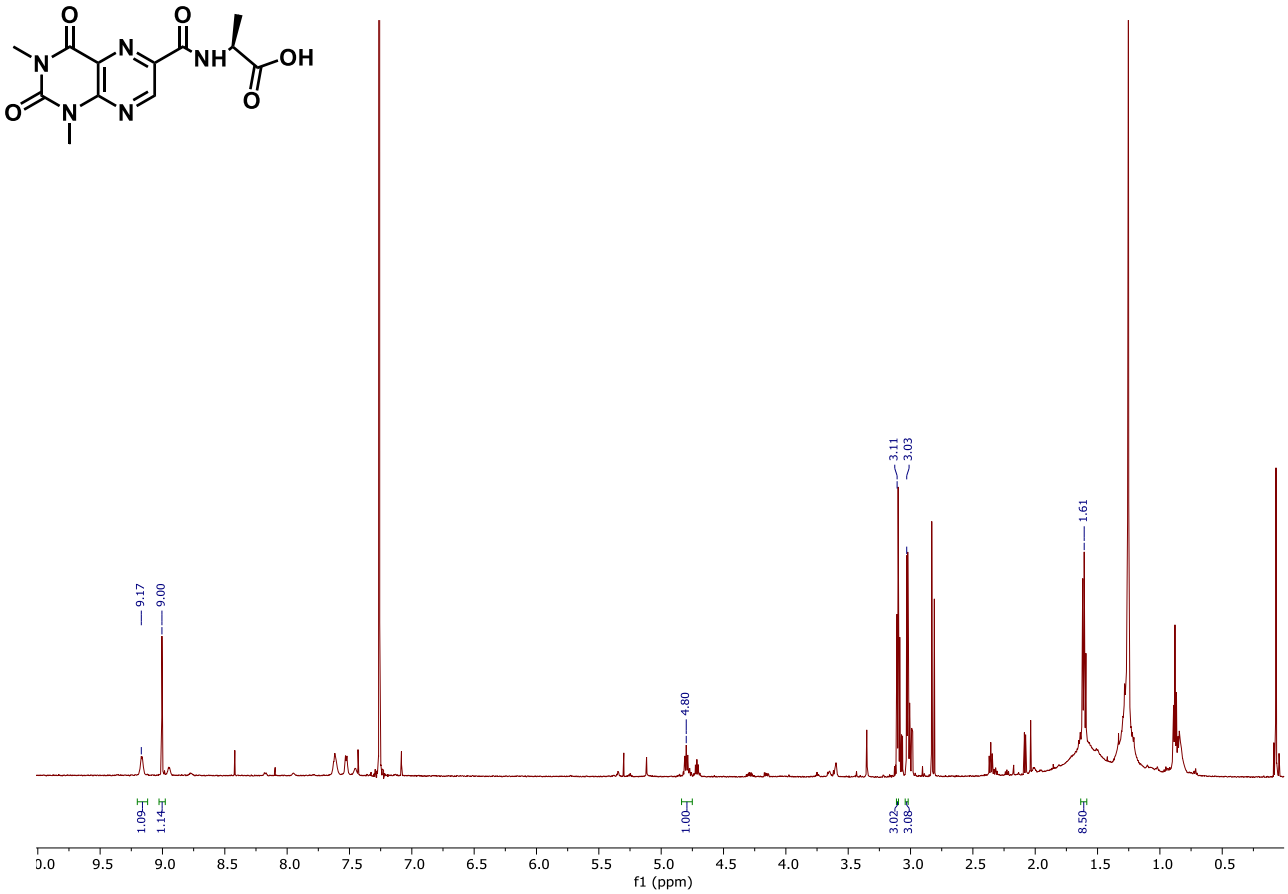
O
O
N
NH
OH
O
N
O
N
N
9.17
9.00
4.80
3.11
3.03
1.61
1.09
1.14
1.00
3.02
3.08
8.50
f1 (ppm)

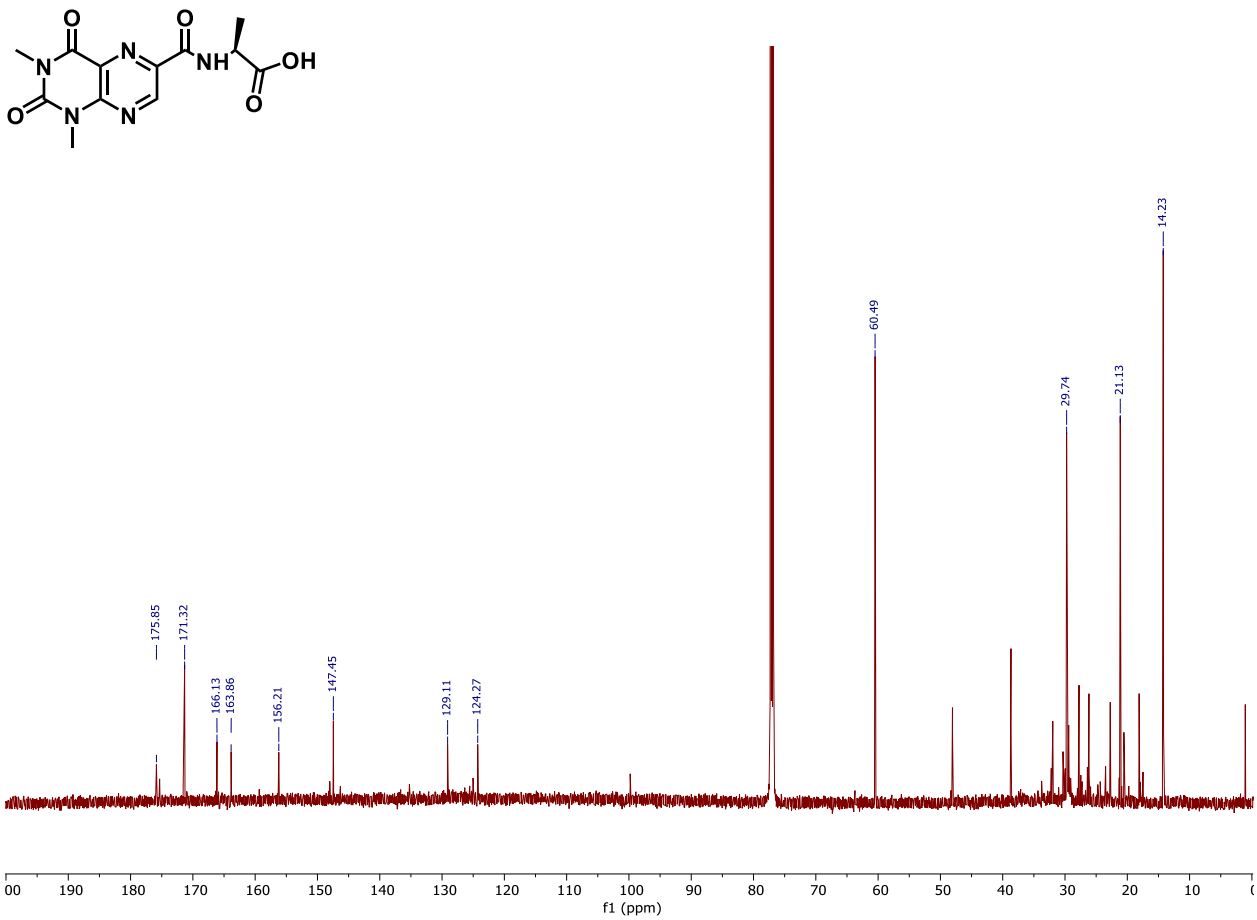
O
O
N
NH
OH
O
N
O
N
N
175.85
171.32
166.13
163.86
156.21
147.45
129.11
124.27
60.49
29.74
21.13
14.23
f1 (ppm)

5. References

[1] A.M Valdes, J. Walter, E. Segal, T.D. Spector, *BMJ*, **2018**, 361.

[2] Y.J. Zhang, S. Li, R.Y. Gan, T. Zhou, D.P. Xu, H.B. Li. *Int. J. Mol. Sci.* **2015**, 16(4), 7493-7519.

[3] R.I Aminov. *Front. Microbiol*., **2010**, *1*, 1-7.

[4] C. L Ventola, *Pharm Thera.*, **2015**; *40* (4), 277-283.

[5] S.E. Rossiter, M.H. Fletcher, W. M. Wuest. *Chem Rev.* **2017,** *117*(19), 12415–12474.

[6] Centers for Disease Control and Prevention (U. S.), *Methicillin-resistant Staphylococcus aureus*, **2019**.

[7] Centers for Disease Control and Prevention (U. S.), *Antibiotic Resistance Threats in the United States*, **2019**.

[8] A. R. Mahoney, M. M. Safaee, W. M. Wuest, A.L. Furst, *iScience*, **2021**, *24*, 102304.

[9] C. Murray et al., *Lancet*, **2022**, *399*, 629-655.

[10] R. E. Dixon, R. A. Kaslow, D. C. Mackel, C. C. Fulkerson, G. F. Mallison, *JAMA* **1976**, *236*, 2415–2417.

[11] S. Alkhalifa, M. C. Jennings, D. Granata, M. Klein, W. M. Wuest, K. P. C. Minbiole, V. Carnevale, *ChemBioChem*, **2020**, *21*, 1510–1516.

[12] M. Okada, T. Sugita, C. P. Wong, T. Wakimoto, I. Abe, *J. Nat. Prod.* **2017**, *80*, 1205–1209.

[13] K. R. Morrison, R. A. Allen, K. P. C. Minbiole, W. M. Wuest, *Tetrahedron Lett.* **2019**, 60, 150935.

[14] M. A. Garrison, A. M. Mahoney, W. M. Wuest, *ChemMedChem*, **2021**, *16*, 463-466.

[15] L. Peng, J. DeSousa, Z. Su, B. M. Novak, A. A. Nevzorov, E. R. Garland, C. Melander, *Chem. Commun.* **2011**, *47*, 4896–4898.

[16] C. Wang, X. Wu, H. Bai, K.H. Zaman, S. Hou, J. Saito, S. Wongwiwatthananukit, S. Kim, S. Cao. *J. Nat. Prod.*, **2020**, *83*, 2233−2240.

[17] B. Daniels, F. Li, D. Furkert, M. Brimble, *J. Nat. Prod.*, **2019** *82* (7), 2054-2065.

[18] K.L. Chew, M. La, R. Lin, J. Teo. *J. Clin. Microbiol*, **2017**, *15* (9), 2609-2616.

[19] J. Casanova, N. D. Werner, R. E. Schuster, *J. Org. Chem.*, **1966**, *31* (11), 3473-3482.
L. Wang, M. Zhu, Q. Zhang, X. Zhang, P. Yang, Z. Liu, Y. Deng, Y. Zhu, X. Huang, L. Han, S. Li, J. He, *ACS Chem. Biol.*, **2017**, *12*, 3067-3075.

[20] G. E. Kenny, A. C. Rosenzweig, *Annu. Rev. Biochem*, **2018**, *87*, 645-676.

[21] J.A. Shapiro, K.R. Morrison, S.R. Chodisetty, D.G. Musaev, W.M. Wuest, *Org. Lett.* **2018,** *20,* 5922-5926.

[22] I. Hübner, J. A. Shapiro, J. Hoßmann, J. Drechsel, S. Hacker, P. Rather, D. Pieper, W. M. Wuest, S. Sieber. *ACS Cent. Sci.*, **2021**, *7* (3), 488-498.

[23] F. F. Blicke, H. C. Godt, *J. Am. Chem. Soc.*, **1954**, *76* (10), 2798-2800.

[24] F. Yoneda, R. Koga, *J. Heterocyclic Chem.*, **1982**, *19*, 949-951.

[25] Y. Si, P. Zhu, S. Zhang, *Org. Lett.*, **2020**, *22*, 9086-9090.